Journal of
Medicinal Chemistry



Article

# Synthesis of Novel Potent Archazolids: Pharmacology of an Emerging Class of Anticancer Drugs

Stephan Scheeff, Solenne Rivière, Johal Ruiz, Aliaa Abdelrahman, Anna-Christina Schulz-Fincke, Meryem Köse, Felix Tiburcy, Helmut Wieczorek, Michael Gütschow, Christa E Müller, and Dirk Menche

*J. Med. Chem.*, **Just Accepted Manuscript** • DOI: 10.1021/acs.jmedchem.9b01887 • Publication Date (Web): 28 Jan 2020



## Just Accepted



is published by the American Chemical Society. 1155 Sixteenth Street N.W., Washington, DC 20036

# Synthesis of Novel Potent Archazolids: Pharmacology of an Emerging Class of Anticancer Drugs

*Stephan Scheeff,[†] Solenne Rivière,[†] Johal Ruiz,[†] Aliaa Abdelrahman,[‡] Anna-Christina Schulz-Fincke,[‡] Meryem Köse,[‡] Felix Tiburcy,[§] Helmut Wieczorek,[§] Michael Gütschow,[‡] Christa E. Müller,[*‡] and Dirk Menche[*†]*

[†]Kekulé-Institut für Organische Chemie und Biochemie, Universität Bonn, Gerhard-Domagk-Str. 1, D-53121 Bonn, Germany

[‡]Pharmazeutisches Institut, Universität Bonn, An der Immenburg 4, D-53121 Bonn, Germany

[§]Universität Osnabrück, Fachbereich Biologie/Chemie, D-49069 Osnabrück, Germany.

**Abstract:** V-ATPase has recently emerged as a promising novel anticancer target based on extensive *in vitro* and *in vivo* studies with the archazolids, complex polyketide macrolides which present the most potent V-ATPase inhibitors known to date. Herein, we report a biomimetic, one-step preparation of archazolid F, the most potent and least abundant archazolid, the design and synthesis of five novel, carefully selected archazolid analogs, and the biological evaluation of these antiproliferative agents leading to the discovery of a very potent but profoundly simplified archazolid analog. Furthermore, a first general biological profiling of the archazolids

against a broad range of more than 100 therapeutically relevant targets is reported, leading to the discovery of novel and important targets. Finally, first pharmacokinetic data of these natural products are disclosed. All of these data are relevant in the further preclinical development of the archazolids as well as the evaluation of V-ATPases as a novel and powerful class of anticancer targets.

## INTRODUCTION

Vacuolar type ATPases (V-ATPases) constitute heteromultimeric proton translocating proteins that are localized in a multitude of eukaryotic membranes.[1] They are responsible for retaining the cellular pH homeostasis and play an important role in the control of receptor-mediated recycling.[2] V-ATPases also regulate membrane trafficking, facilitate protein degradation and neurotransmitter release[2b] and are involved in urinary acidification,[3] bone resorption[4] and sperm maturation[5] and have recently also been implicated in the regulation of cholesterol biosynthesis[6] and cytokine secretion.[7] Consequently, a malfunction or overexpression of these enzymes has been associated with various diseases,[1a,8] which renders the development and understanding of molecular determinants of potent inhibitors an important research goal from the perspective of medicinal chemistry. The natural macrolides archazolids A (**1**) and B (**2**, Figure 1) represent the most potent V-ATPase inhibitors known to date with activities in the low nanomolar range.[9] On a molecular level, they bind selectively to the functional transmembrane subunit c in a non-covalent fashion.[10,11] Recently, the archazolids have become very valuable chemical tools to evaluate the potential of V-ATPases in anticancer therapies[12] and based on these and other studies,[13] V-ATPases have been increasingly emerging as promising novel anticancer targets. In detail, inhibition by archazolid abrogates tumor metastasis via inhibition of endocytic activation,[12a] leads to impaired cathepsin B activation *in vivo*,[12c] modulates anoikis resistance and

metastasis of cancer cells,[12d] overcomes trastuzumab resistance of breast cancers,[12e] blocks iron metabolism and thereby mediates therapeutic effects in breast cancers,[12f] and plays a role in tumor-sensitizing in the context of the MDM2 antagonist nutlin-3a.[12g] Recently, a model of cell-death induction by archazolid-mediated V-ATPase inhibition has been proposed.[12b]

However, only limited structure-activity relationship studies (SAR),[9,14] little information on additional biological targets[15] and no pharmacokinetic data have been reported for the archazolids. The very low natural supply and lack of a synthetic route to the archazolids have impeded a detailed biological evaluation of this promising class of polyketides.

Recently, archazolid F (**3**), has been discovered as a more potent natural analog, which bears a 3,4- instead of the 2,3-olefin substructure of parent compound **2**.[16] However, the very low natural supply to **3** as well as the lack of synthetic routes to corresponding archazolid derivatives like unknown archazolids **4**-**8** have impeded a detailed biological evaluation.

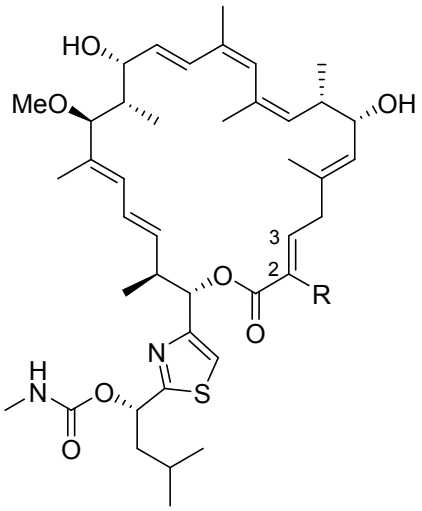

**1**: Archazolid A (R = Me)
**2**: Archazolid B (R = H)

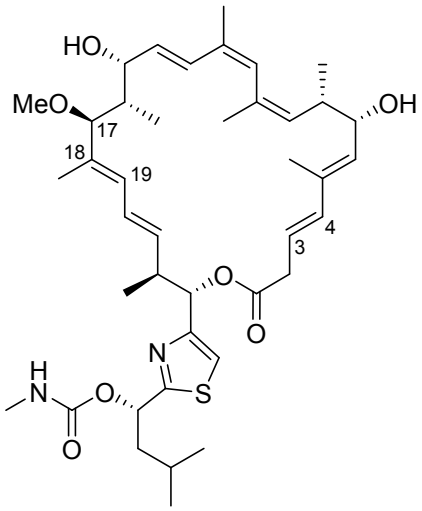

**3**: Archazolid F

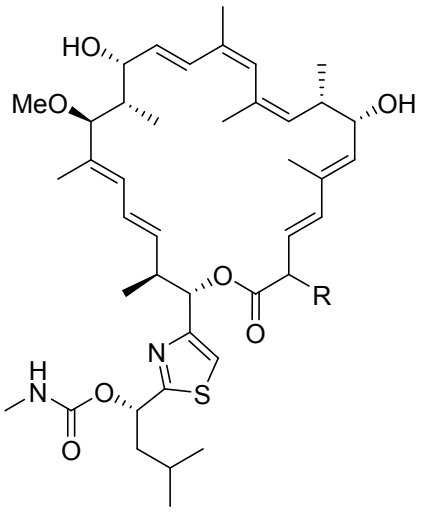

**4**: *iso*-Archazolid $A_1$ (R = Me)
**5**: *iso*-Archazolid $A_2$ (R = Me)

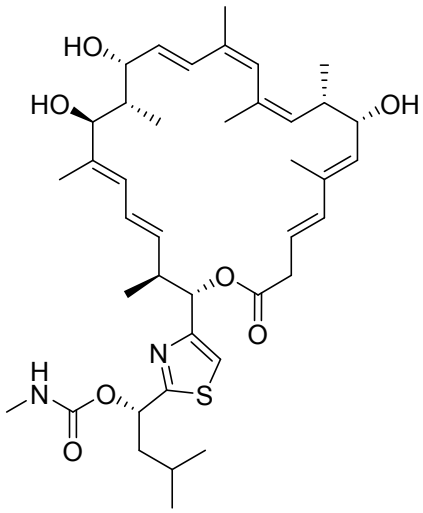

**6**: desmethyl-Archazolid F

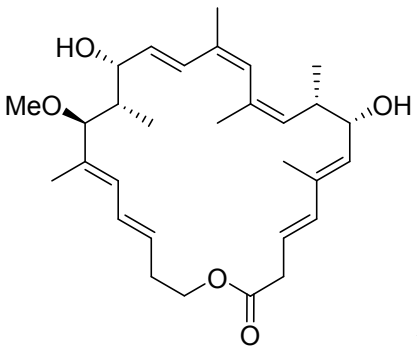

**7**: Archazolog

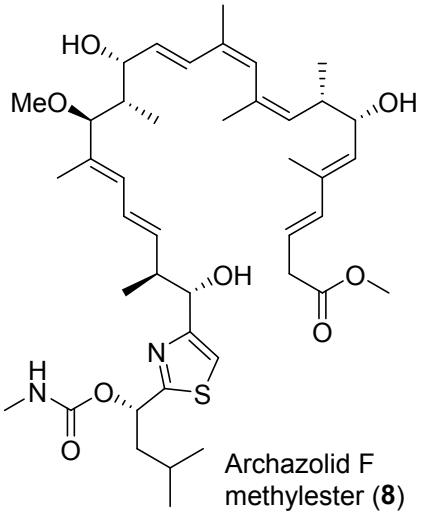

Archazolid F methylester (**8**)

**Figure 1.** Known archazolids A, B and F, an emerging class of potent V-ATPase inhibitory anticancer drugs, and novel archazolids **4**-**8**, discussed herein.

One total synthesis of archazolid A (**1**)[17a] and two syntheses of archazolid B (**2**)[17b,c] as well as several fragment syntheses of 2,3-dihydroarchazolid B[18] have been reported.[17e] However, these routes could not be adapted for large scale or analog synthesis and consequently, only limited SAR data are available, relying purely on derivatization[10,14a,f,g] or acyclic fragments.[14e,18] To circumvent these limitations, we have recently designed a novel route and successfully implemented this approach for a first total synthesis of archazolid F.[17d] Key features include a scalable synthesis of the Northern subunit and its connection to the Southern part by a stereoselective aldol condensation to forge the C18-C19 olefin and a ring closing metathesis reaction along the C3-C4 bond. This modular strategy allows for a direct replacement of the Southern part and modulation of the North-Western region.

Concerning their pharmacology - besides V-ATPase inhibition -, there has only been a single report by the group of Schneider who developed an *in silico* method for determination of molecular targets and thereby discovered four previously unknown biological interaction sites, two nuclear receptors (PPARγ and FXR) activated by **1** and two lipid-metabolizing enzymes (5-lipoxygenase and mitochondrial prostaglandin E synthase-1 (mPGES-1)) inhibited by **1**.[15] However, the effects were weak (moderate activation of PPARγ and FXR, incomplete inhibition of 5-lipoxygenase and mPGES-1 in cell free systems) and the determined $EC_{50}$/$IC_{50}$ values were three orders of magnitude higher as compared to the V-ATPase inhibition leading to the conclusion that they are biologically less significant.

Herein, we report a ~~very~~ concise one-step synthesis of archazolid F (**3**), the most potent and least abundant archazolid, by an efficient isomerization approach, the design and synthesis of five novel, carefully selected archazolid analogs (**4**-**8**) differing in the Southern part of the molecule and the biological evaluation of antiproliferative agents resulting in the discovery of a very potent, but profoundly simplified archazolid analog. Furthermore, we report a first general profiling of the archazolids towards a broad range of more than 100 therapeutically relevant targets leading to the discovery of four novel and therapeutically important targets. Finally, we disclose first pharmacokinetic data of this powerful class of emerging anticancer agents.

## RESULTS AND DISCUSSION

**One-step synthesis of archazolid F (3) and of *iso*-archazolids $A_1$ (4) and $A_2$ (5).** Presumably,[16,19] archazolid F is biosynthetically derived from archazolid B by an isomerization or directed migration of the C2-C3 double bond towards the C3-C4 position.[16] Based on this analysis, we have recently realized a stepwise base-mediated ring opening, isomerization and lactonization of archazolid B towards archazolid F.[17d] Within this study, we now evaluated, whether suitable conditions could also be established for a direct conversion of archazolid B to F (Scheme 1). After evaluation of a broad range of bases (*i.a.* KHMDS, LDA, BuLi, histidine), this could indeed be realized and a direct, efficient migration procedure could be developed. Mechanistically, this conversion may be initiated by a 1,4-addition of DBU to the enoate followed by an elimination of the resulting adduct towards generation of the 3,4-alkene. Also, an ene-type reaction may be possible.[20] The protocol utilizes DBU in THF and proceeds in excellent yields, both with DBU in excess (90%, 20h, Scheme 1a) as well as with only catalytic amounts of the base (97%, 9 days). Notably, no traces of a likewise possible double bond migration from

the 5,6- to the 4,5-position was observed, even though this product may benefit from additional enoate stabilization. This procedure proved general and could then be successfully applied also to the divergent conversion of archazolid A to *iso*-archazolids $A_1$ (**4**) and $A_2$ (**5**). The configuration of **4** and **5** were assigned by NMR methods in combination with molecular modeling. Minor amounts of reisolated starting material (13%) were also obtained. Archazolids **4** and **5** interconvert in slightly acidic or basic media. They are stable under neutral conditions. Diastereomeric purity was confirmed in all cases by full NMR assignments and HPLC analyses. Notably, these diastereoisomeric compounds show almost same MS spectra but elute at different times in the HPLC chromatograms (i.e., 14.5 and 16.6 min, respectively). Likewise, archazolid B and F gave similar MS but different retention times (14.5 and 15.1 min) in the HPLC, consistent with isomeric structures, which were readily assigned by conventional 2D-NMR methods, as previously described.[16] The determination of the newly generated stereocenter of *iso*-archazolid $A_1$ (**4**) and $A_2$ (**5**) could be accomplished by NOE measurements of the α proton and the associated methyl group in comparison with before calculated structures (for full NMR assignment of all new compounds, see SI section).

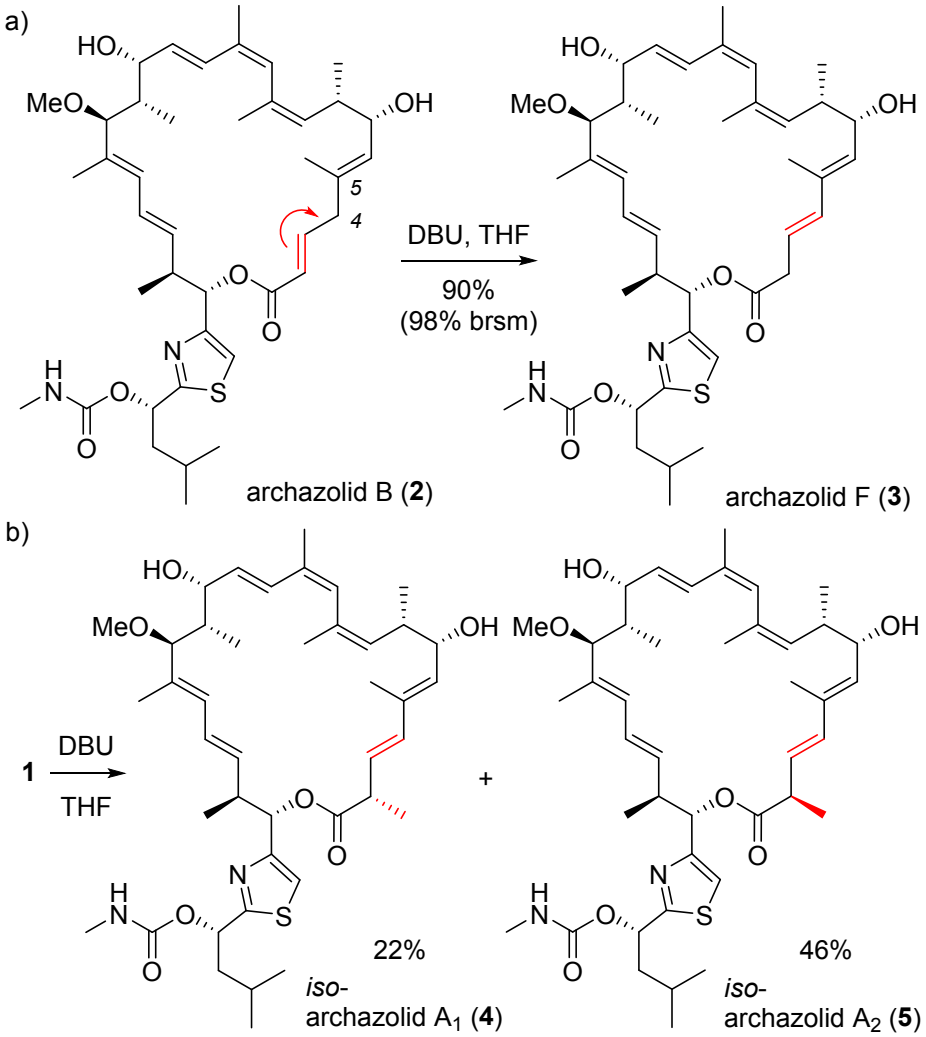


**Scheme 1.** Biomimetic synthesis of archazolid F by a DBU mediated isomerization of the C2-C3 double bond (a) and application of this strategy for synthesis of *iso*-archazolids $A_1$ and $A_2$ (b).

**Design and total synthesis of archazolid F analogs.** Existing *in vivo* studies with the archazolids have revealed surprisingly low toxic effects in mice model, despite very potent antiproliferative activities in a number of anticancer cell lines.[12] In order to analyze whether this may be explained by the low pharmacokinetic stability of the archazolids, involving a rapid demethylation, as revealed within this study (see below), we targeted desmethyl-archazolid F (**6**). Based on further analysis of an earlier modeling study, demethylation would also directly influence the hydrogen bonding ability of the C15 to C17 which has been predicted to be of

crucial importance for target binding.[14g] As shown in Scheme 2, desmethyl-archazolid F (**6**) was obtained from fragments **11** and **9** by application of strategies recently developed in our group.[17d] While Northern part **11** was prepared by previous protocols,[17d] Southern subunit **9** was prepared by protection and cross metathesis of known compound **10**.[17] Fragment coupling was then accomplished by an aldol condensation, involving a lithium-mediated coupling and a two-step elimination with DBU via an acetate intermediate. Essentially full stereoselectivity towards *E*-configured enone **12** was observed, demonstrating the general usefulness of this previously established protocol.[17d] No epimerization of the methyl group at C16 by deprotonation at this kinetically less accessible position was observed. After selective cleavage of the TES-ether and butanoate attachment, reduction of the ketone with $NaBH_4$ proceeded in useful selectivity (*dr* 5:1).[17b] Finally, RCM reaction of resulting diene-ene **13** with catalyst **14**[21] and global deprotection liberated desmethyl-archazolid F (**6**) in 24% yield after HPLC separation.

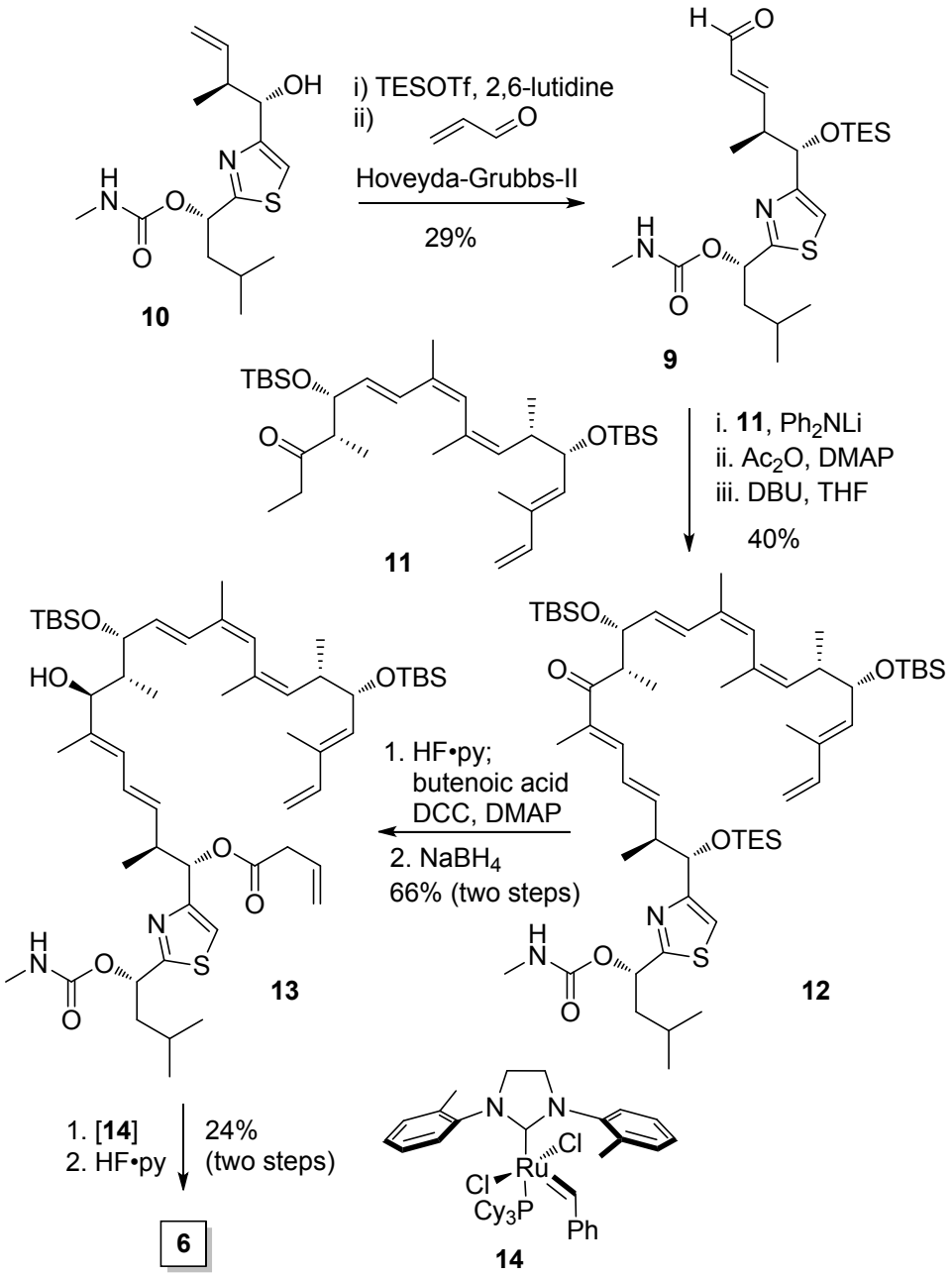


**Scheme 2.** Total synthesis of desmethyl-archazolid F (**6**).

Based on mutagenesis and crosslinking studies,[10] in combination with molecular modeling and supported by EPR measurements,[11] a framework for the molecular archazolid interactions with V-ATPase had been proposed.[14g]

Based on a detailed reevaluation and analysis of these target-inhibitor interactions[10,11,14a,14g] a pharmacophore model is now proposed. In detail, as shown in Figure 2, the methyl groups at C-2 (in the case of archazolid A), 5, 10, 12 and 16 are in close proximity to residues Y66, I134, F135, E137, V138 and L141 due to hydrophobic interactions. Notably, the methyl group at C-22 is not directed towards the protein. Another hydrophobic interaction was observed between the C1-C6 moiety and the Y66 residue of the protein. A hydrogen bond between C-7-OH and I134 could be the key interaction for the inhibition of V-ATPase. Furthermore C-15-OH showed a close proximity to Y142. One of the methyl groups of the *iso*butyl group of the archazolid side chain only interacts weakly with the *iso*butyl group leucine L144 and likely plays an inferior role in V-ATPase inhibition. Therefore, a binding pocket of the c-subunit of V-ATPase is proposed, which is centered around the North-Eastern moiety of the macrocycle. Importantly, this analysis is agreement with limited SAR data available so far (see: Supporting Information section).

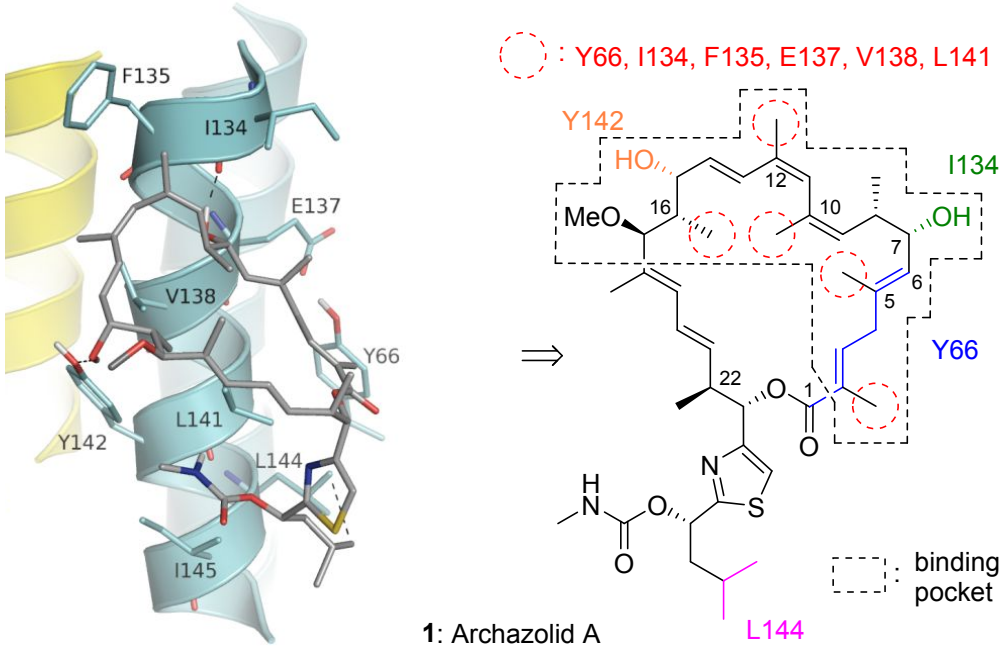


**Figure 2.** Proposed V-ATPase binding pocket of the archazolid A.

Accordingly, it was rationalized that the Northern part would be critical for target interaction presumably as recognition domain while more flexibility was suggested for the Southern region. Consequently, our simplification strategy concentrated on this area. Complete removal of the thiazole and the neighboring methyl center was planned and truncated archazolog **7** was targeted. For its synthesis we applied again the same modular strategy, which had been designed for a facile modulation of Southern fragments with retention of the Northern pharmacophore.[17d] As shown in Scheme 3, required aldehyde **15** was obtained from commercial **16** by complete reduction to the diol, selective allylic oxidation ($MnO_2$) and TBS protection of the derived hydroxyaldehyde **17**. Aldol condensation with ketone **11** following our three step protocol then proceeded with excellent yields (92%) demonstrating the high usefulness of this procedure for analog preparation. The resulting enone **18** was reduced stereoselectively ($NaBH_4$, *dr* >8:1) followed by methylation yielding **19** with 83% over two steps. After selective deprotection of the primary TBS ether and coupling to ester **20**, the archazolog synthesis was finalized by RCM with **14** and global deprotection.

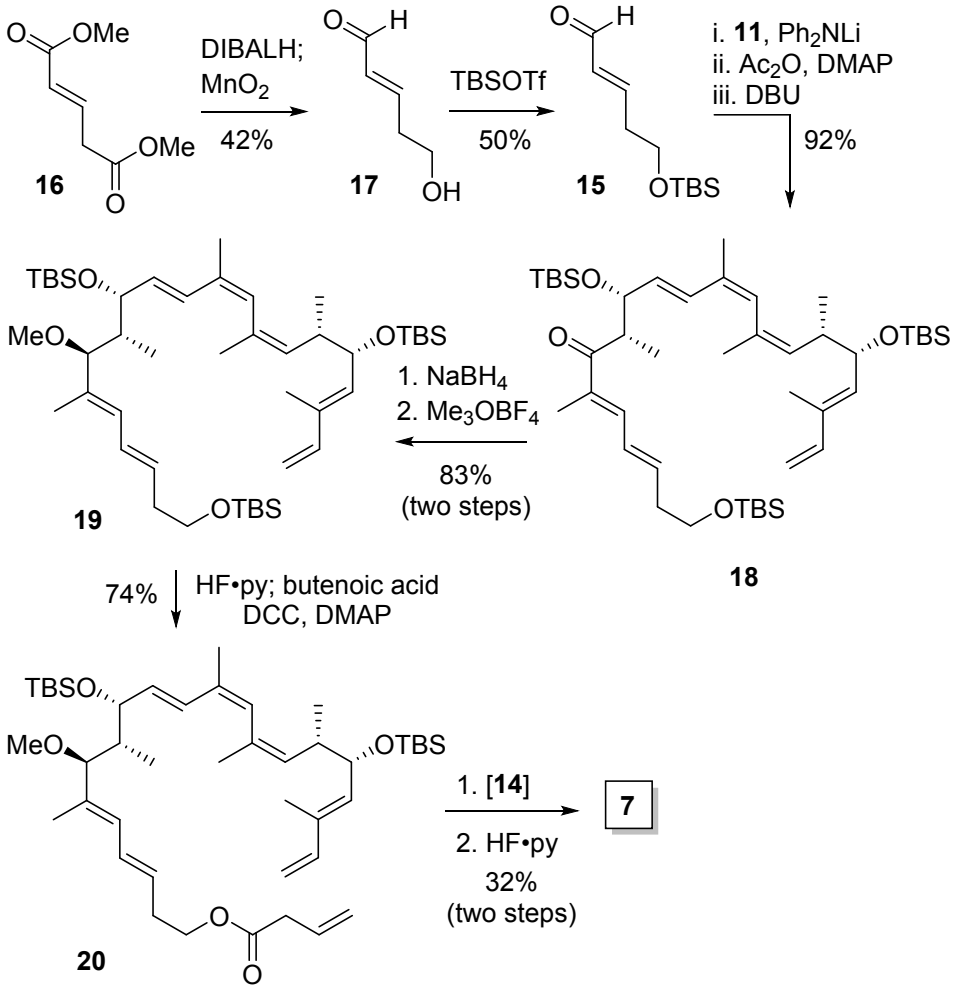


**Scheme 3.** Total synthesis of simplified archazolog **7**.

Finally, the opened archazolid F methyl ester **8** was required in order to study the general importance of the macrocyclic ring as well as to further analyze the biological role of the Southern part. Importantly, the *in silico* approach by the group of Schneider for analysis of the pharmacology of the archazolids relied on fragment analysis, without consideration of the biological importance of the macrocyclic ring.[15] Furthermore, also the analog studies of O'Neil relied on acyclic compounds.[14e,18] In order to address this issue we targeted acyclic analog **8**. As previously reported[17d] and shown in Scheme 4, a LiOH mediated protocol with archazolid B (**2**)

was applied, which was accompanied by α,β to β,γ-enoate isomerization,[17d,19] giving **8** after stabilization as a methyl ester (81%).

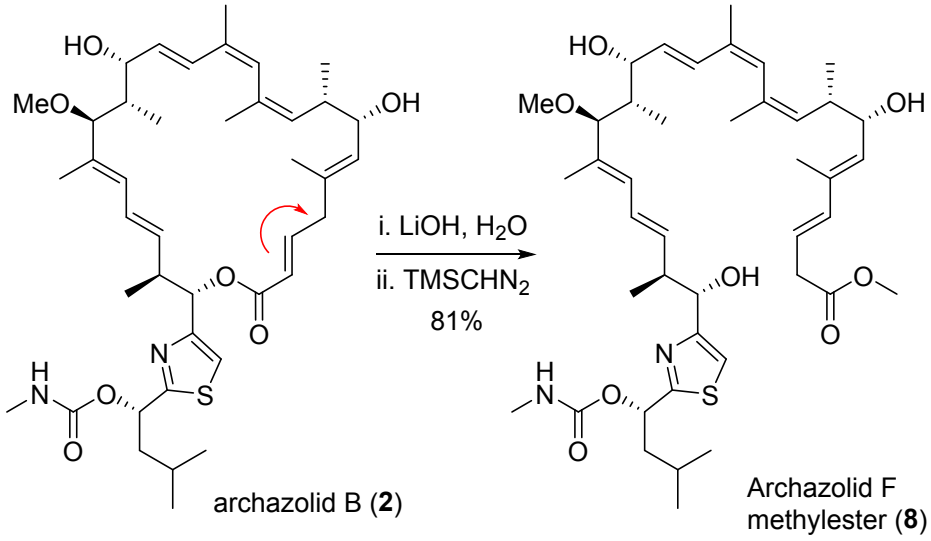


**Scheme 4.** Synthesis of archazolid F methyl ester (**20**) by opening of archazolid B (**2**).[17d]

**Purity of the compounds**

Purity of the final products including diasteromeric purity was confirmed by NMR measurements with full assignments and by HPLC-UV/ESI-MS analyses, in addition to the measurement of optical rotation. All compounds were purified by HPLC before biological measurements and showed a purity of >95% (For details, see Experimental Section and Supporting Information).

**Biological Evaluation.** We first evaluated the antiproliferative activities of these novel archazolids by analyzing their effects on the growth of 1321N1 astrocytoma cells, a human brain cancer cell line, in direct comparison to the parent natural products as well as to bafilomycin (**21**), which is also a well-known inhibitor of V-ATPase. As shown in Table 1, novel archazolid F (**3**) and *iso*-archazolids $A_1$ (**4**) and $A_2$ (**5**) showed very high potencies in the low nanomolar

range, demonstrating that a certain structural flexibility within the C2-C4 subunit appears to be tolerated. Importantly, with an activity in the subnanomolar range, simplified archazolog **7** essentially retained the activity of the parent natural products, which demonstrates that the thiazole side chain may be removed without loss of potency. In contrast, removal of the C17-methyl ether leads to considerable loss of activity (*viz* compound **6**), showing the importance of the Northern region for the pharmacophore, further confirming our hypothesis. Likewise, the macrocyclic core was shown to be significant for potency as a ring-opened analog was much less active. This will be of importance for future biological studies targeting linear fragments[14e,18] as well as *in silico* approaches.[15] Likewise, the compounds exhibited very potent to moderate V-ATPase inhibitory profiles. The new *iso*-archazolids $A_1$ (**4**) and $A_2$ (**5**) as well as archazolid F (**3**) displayed activities equipotent to the parent natural products (Table 1), which also confirms an initial biological study of **3**,[16] while ring opened analog **8** was less potent. However, archazolid A (**1**), B (**2**) and simplified analogue **7** were significantly more potent in inhibiting astrocytoma cell proliferation than V-ATPase activity (25-fold, 117-fold and 545-fold respectively), while the other compounds showed similar $IC_{50}$ values in both assays except for desmethyl-archazolid F (**6**) which will be discussed below. Potentially, the different activities of **1**, **2** and **7** in these assays (inhibition of V-ATPase from the moth *Manduca sexta* vs. toxicity towards human astrocytoma cells) may arise from interaction with additional molecular targets in the cancer cell line or result from the different species used in these two assays. These data reveal archazolog as a highly potent but dramatically simplified archazolid, confirming our design and pharmacophore model. This profound biological potency is quite remarkable, as only few such examples have been described for complex natural products.[22] In comparison, desmethyl-archazolid **6** and ring-opened structure **8** inhibited V-ATPase with similar potency ($IC_{50}$: : 213

nM; **8**: 352 nM), however exhibiting highly reduced antiproliferative activity. Given the promiscuous biological potency that is frequently observed for natural products, we were then searching for alternative targets. In contrast to the aforementioned *in silico* approach,[15] we opted for a biological screening and submitted a 10 μM solution of archazolid A (**1**) to a general profiling towards a broad range of more than 100 therapeutically relevant targets, including a broad panel of G-protein-coupled receptors (GPCRs) and nuclear receptors. In addition, various ion channels including ligand-gated ion channels, enzymes and a broad variety of kinases were evaluated (see SI section). No activity against a broad range of kinases were detected and previously it has been found that archazolid does not inhibit F- and P-ATPases.[9b] While no effects were detected for the majority of the targets at a high test concentration of 10 μM, relevant interactions were observed with only five biological systems, demonstrating high selectivity. In detail, as shown in Table 2, archazolid A (**1**) was found to be a potent ligand of the human $A_3$ adenosine receptor ($K_i$ 967 nM), a proposed anti-cancer target[23] (Table 2, entry 1), while it did not interact with the other adenosine receptor subtypes ($A_1$, $A_2A$ and $A_2B$). Secondly, archazolid A (**1**) proved to be an efficient inhibitor of the PPARγ receptor (entry 2), in agreement with the previous finding.[15] Moreover, archazolid A (**1**) demonstrated moderately potent inhibitory effects on the $Ca^{2+}$-channel (entry 3). The target at which **1** showed its highest potency was the P2X3 receptor ($IC_{50}$ 86.1 nM), an ATP-gated ion channel receptor, that is associated with cancer progression and cancer-induced pain.[24] Thus, the blockade of P2X3 receptors by archazolid A may contribute to its anti-cancer effects. Only a 4-fold lower potency was observed for archazolid A as an inhibitor of leukocyte elastase.

Table 1. Biological data of archazolids **1**-**3**, novel analogs **4**-**8**, in comparison to bafilomycin (**21**).[a]

| | Growth inhibition of 1321N1 astrocytoma cells:[b] $IC_{50}$ ± SEM [nM] | V-ATPase inhibition $V_1/V_o$ holoenzyme: $IC_{50}$ ± SD [nM] | Human P2X3 inhibition: $IC_{50}$ ± SEM[nM] | Affinity for the human adenosine $A_3$ receptor:[c] $K_i$ ± SEM [nM] | Human leukocyte elastase inhibition $IC_{50}$ ± SEM [nM] |
|---|---|---|---|---|---|
| **1** | 0.253 ± 0.096 | 6.33 ± 2.18 | 86.1 ± 17.7 | 967 ± 186 | 352 ± 50 |
| **2** | 0.145 ± 0.052 | 17[d] | 353 ± 38 | 1180 ± 170 | 316 ± 126 |
| **3** | 4.51 ± 0.51 | 6.26 ± 1.33 | 438 ± 144 | 859 ± 75 | 830 ± 134 |
| **4** | 2.16 ± 1.057 | 5.52 ± 1.45 | 648 ± 184 | 1140 ± 389 | 721 ± 83 |
| **5** | 2.58 ± 2.58 | 7.94 ± 3.08 | >2000 | ≥ 10000 | 595 ± 89 |
| **6** | 3050 ± 230 | 213 ± 85 | >10000 | 1376 ± 739 | 1540 ± 148 |
| **7** | 0.757 ± 0.121 | 413 ± 53 | 1310 ± 190 | 609 ± 39 | 5850 ± 1560 |
| **8** | 296 ± 55 | 352 ± 69 | >10000 | 1611 ± 270 | 2340 ± 464 |
| **21** | 3.06 ± 0.98 | 10[e] | 755 ± 246 | 1080 ± 170 | n.i.[f] |

[a] At least, three separate experiments were performed in all cases. [b] Growth inhibition was determined in the MTT assay Ref. [25]; [c] determined in radioligand binding assays at Chinese hamster ovary cell membrane preparations recombinantly expressing the human $A_3$ adenosine receptor versus [$^3$H]PSB-11 as a radioligand. [d] Value taken from Ref. [14f]. [e] Value taken from Ref. [26].[f] n.i.: no inhibition.

Table 2. Novel molecular targets of archazolid A (**1**).[a]

| Entry | Target | Potency of archazolid A (**1**) |
|---|---|---|
| 1 | Human $A_3$ adenosine receptor: $K_i$ ± SEM [nM] | 967 ± 186 |
| 2 | Human PPARγ receptor: inhibition with 10 μM of **1** | 82%[b] |
| 3 | $Ca^{2+}$ channel: inhibition with 10 μM of **1** | 52%[b] |
| 4 | Human P2X3 inhibition: $IC_{50}$ ± SEM [nM] | 86.1 ± 17.7 |
| 5 | Human leukocyte elastase inhibition: $IC_{50}$ ± SEM [nM] | 352 ± 50 |

[a] At least three separate experiments were performed. [b] Percent inhibition at indicated concentration of archazolid A.

Based on this initial evaluation we decided to analyze it on the most promising archazolid targets, the purinergic receptors, in more detail. Accordingly, when archazolid A was evaluated on a broad range of nucleotide-activated purinergic receptors, it was found to exhibit very high antagonistic potency specifically for the P2X3 receptor while being inactive at the other human purinergic receptor subtypes $P2Y_1$, $P2Y_2$, $P2Y_4$, $P2Y_6$, $P2Y_{11}$, $P2Y_{12}$, $P2Y_{14}$, GPR17, P2X1, P2X2, P2X3, P2X4, and P2X7 at a high concentration of 10 μM.

Next we investigated the other archazolids for interaction with the P2X3 receptor. As depicted in Table 1, beside archazolid A (**1**, $IC_{50}$ 86.1 nM), archazolid B (**2**, 353 nM) and F (**3**, 438 nM), as well as *iso*-archazolid $A_1$ (**4**, 648 nM) were also potent inhibitors of the P2X3 receptor and likewise showed inhibitory effects in the nanomolar range, although somewhat weaker than archazolid A. Archazolog (**7**, 1.31 μM) still showed a moderate inhibition whereas **5** and **6** appeared to be less potent ($IC_{50}$ >2000 nM) indicating stereoselectivity in binding to the receptor. SARs also indicated that a methyl group in the 2-position of the archazolid scaffold was beneficial when attached to the sp2-hybridized carbon (compare **1** and **2**). Shifting the double bond to the 3,4-position was well tolerated with almost no change in P2X3-inhibitory potency (compare **2** and **3**). However, in that series, a 2-methyl group did not increase potency, which can be explained by the different sterical arrangements in compounds **3**, **4** and **5** ($sp^3$-hybridized C2-atom), and only the *S*-configurated stereoisomer (**4**) was tolerated. This remarkable configuration dependency of activity, which was not observed for the effects on astrocytoma cells and V-ATPase, may be explained by different interactions with the (allosteric) binding site on the P2X3 receptor (see below), which appears to be more sensitive towards the steric arrangement at this

stereocenter, which can also induce or stabilize different conformations of the macrocycles as evidenced by NMR measurements.

We subsequently evaluated the effects of the most potent archazolid A (**1**) on the human P2X3 receptor in more detail. In particular, we were interested in determining whether the archazolids would interact with the orthosteric ATP binding sites on the P2X3 receptor which could enable docking studies since the binding site of ATP is known.[27] To this end the concentration-dependent activation of the P2X3 receptor by ATP in the absence and in the presence of two different concentrations of archazolid A was determined (Figure 3a). The $EC_{50}$ of the P2X3 agonist ATP was unaltered in the presence of archazolid A, but its maximal effect was decreased by archazolid A in a concentration-dependent manner indicating that archazolid A is likely to act as a non-competitive antagonist or negative allosteric modulator of the P2X3 receptor.[28] To further investigate whether the archazolids interact with the ATP binding site on the P2X3 receptor, competition binding studies were performed using [$^{35}$S]ATPγS as a radioligand. Binding curves for ATP and archazolid B (**2**) are displayed in Figure 3b. While ATP showed a concentration-dependent inhibition of [$^{35}$S]ATPγS binding to the orthosteric binding site on the P2X3 receptor with a $K_i$ value of 20.1 ± 0.3 nM, archazolid B did not interfere with [$^{35}$S]ATPγS binding even at high concentrations. These data confirm that archazolid B is a non-competitive P2X3 antagonist acting as a negative allosteric modulator. A direct interaction with the ATP binding sites on the P2X3 receptor can be excluded.

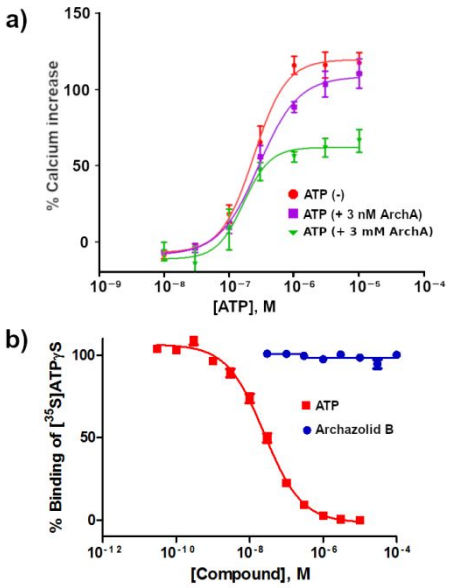


Figure 3. (a) ATP-induced intracellular calcium levels in 1321N1 astrocytoma cells stably transfected with the human P2X3 receptors, measured in the absence and presence of different concentrations of archazolid A. (b) Competition binding experiments at membrane preparations of 1321N1 astrocytoma cells recombinantly expressing the human P2X3R versus [$^{35}$S]ATPγS (0.2 nM); $K_i$ value for ATP: 20.1 ± 0.3 nM.

Radioligand binding studies of the archazolids and the related bafilomycin at the human $A_3$ adenosine receptor resulted in $K_i$ values of around 1 µM for all investigated derivatives (Table 1), which is significantly higher than its inhibitory potency of V-ATPase. Only archazolog showed a slightly higher potency (609 nM).

Subsequently we studied the effects of archazolid A on five different proteases. Besides the serine protease human leukocyte elastase (HLE), the human cysteine proteases cathepsin B and cathepsin L as well as bovine chymotrypsin and trypsin, both serine proteases, were investigated. As noted in entry 5 (Table 2), archazolid A was shown to be a potent HLE inhibitor with an $IC_{50}$ value of 352 nM, while no effects on the other proteases were observed.

Archazolid B (**2**) was as potent as archazolid A (**1**) against HLE, while archazolid F (**3**) and the derivatives **4** and **5** exhibited a weaker HLE inhibitory activity, but still had $IC_{50}$ values in the nanomolar range (Table 1). We also investigated the influence of archazolids **2**-**5** on the proteolytic activity of human cathepsins B and L as well as bovine chymotrypsin and trypsin. They share the inhibition profile of archazolid A (**1**) and did not inhibit the other proteases. Bafilomycin, in contrast, did not inhibit HLE; even at a concentration of 2.5 μM, more the 95% residual activity was observed.

**Pharmacokinetic properties.** Surprisingly, despite the very promising biological activities of the archazolids no information on their pharmacokinetic properties has been reported. Therefore, the metabolic stability of archazolid B (**2**) and F (**3**) was evaluated (Figure 4). Only low metabolic stability was observed in mouse liver (hepatic intrinsic clearance (Clint): 495 μl/min/mg protein), rat liver (Clint: 301) and human liver microsomes (Clint: 533) for archazolid B (**2**). Half-lives of only 2.8 min, 4.6 min and 2.6 min were determined in these test systems and complete degradation was observed within 15 min. As shown in Figure 4a archazolid F (**3**) showed a slightly higher stability in mouse liver (clint: 271). To further analyze the very low metabolic stability of the archazolids, extended metabolism studies were carried out with archazolid F in mouse and human liver microsomes (Figure 4b) revealing a rapid demethylation, oxidation and hydroxylation. Importantly, desmethyl-archazolid **6** and ring-opened structure **8** demonstrated >200-fold reduced antiproliferative activities, however still inhibited V-ATPase ($IC_{50}$: **6**: 213 nM; **8**: 352 nM). Together with biological data for an oxidized analog,[14a] these

results demonstrate that V-ATPase inhibition may be retained for metabolites, which show dramatically reduced cytotoxicity, and this might explain the low toxic effects of archazolids observed in *in vivo* studies and suggest a prodrug role (or at least a limited prodrug role since the parent compound may still contribute to the activity) for authentic archazolids. This issue indicates that *in vivo* data obtained with archazolid have to be interpreted with great caution, and published data may have to be reevaluated in the light of these new findings.

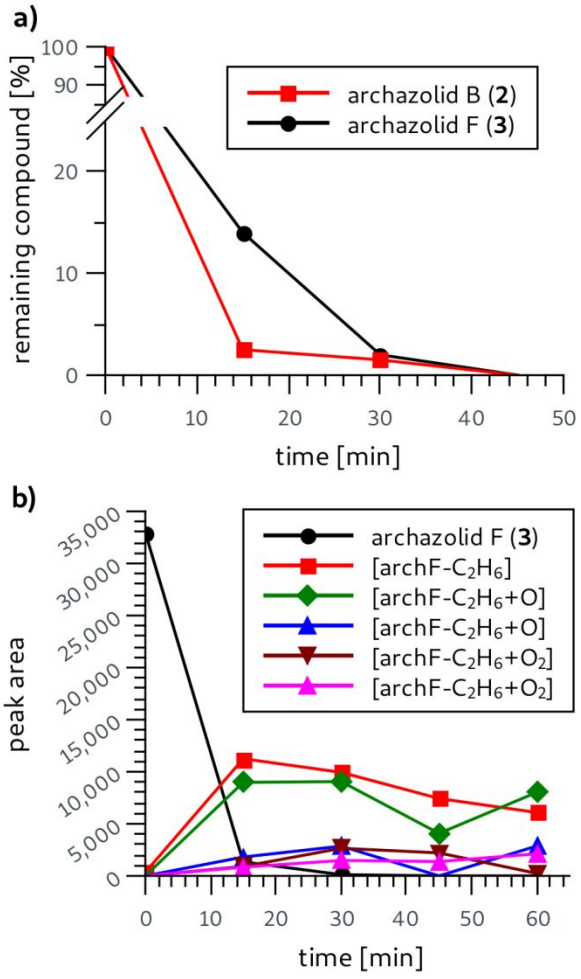


**Figure 4.** Metabolic stability of archazolid B (**2**) and F (**3**): a) metabolic stability in mouse liver microsomes; b) peak areas of archazolid F and metabolites in human liver microsomes.

In addition, the potential of archazolid B to cross the blood brain barrier was analyzed using a modified parallel artificial permeation assay (PAMPA). Following this assay, no penetration was detected, which suggests that no effect on the central nervous system would be expected. Also, no permeability on Caco2 monolayers was observed in a Caco2-permeation assay. Therefore, an intestinal absorption *in vivo* may be difficult to obtain with the parent natural product. The kinetic aqueous solubility of archazolid B was determined to be moderate (1.6 μM). Furthermore, following an optimized protocol for ultrafiltration, archazolid B revealed high plasma protein binding (close to 100%) in mouse, rat and human samples. These data suggest that the parent compound displays unfavorable pharmacokinetic properties. On the other hand this high plasma protein binding may also have a protective effect to stabilize the compound against degradation.

Finally, archazolid B was tested for potential inhibition of six different human cytochrome P450 isoenzymes, CYP1A2, CYP2B6, CYP2C9, CYP2C19, CYP2D6 and CYP3A4, known to be important for drug metabolism. As shown in detail in the SI section, inhibition was moderate at a concentration of 100 nM, while it was somewhat higher at a concentration of 1 μM for three of the enzymes (CYP2C9, CYP2C19, and CYP3A4), however even at that concentration no complete inhibition was observed.

## CONCLUSION

In summary, we have developed an efficient one-step synthesis of archazolid F from archazolid B and reported the design and synthesis of five novel archazolids. This led to the discovery of a novel class of very potent and synthetically more easily accessible archazolid isomers, which are accessible by either an effective biomimetic double bond migration or a

modular total synthesis approach via ring closing metathesis. Desmethyl- and ring-opened archazolids **6** and **8** retained potent inhibitory profiles against key biological targets but demonstrated significantly reduced antiproliferative activities. In addition, a very potent but greatly simplified archazolog (**7**) has been developed which retains full antiproliferative activity of the parent natural products. It is also still active against both V-ATPase and P2X3, however with reduced potency, thus sharing the molecular mode of action of the archazolids. Furthermore, a general biological profiling of archazolid A on more than 100 biologically relevant targets revealed several novel molecular interaction sites. Archazolid A was shown to be a potent inhibitor of the human G-protein-coupled A3-adenosine receptor, the ATP-gated ion channel receptor P2X3, and human leukocyte elastase. In general, a very high specificity for these important biological targets versus closely related proteins was observed. Importantly, this GPCR, ion channel receptor and protease belong to major target classes for drugs, and the three proteins have all been suggested as novel targets in cancer therapy, among other indications. These results also demonstrate the high importance and relevance of conventional biological profiling technologies, as none of these targets have been proposed by an in silico algorithm recently reported, which had led to the discovery of nuclear receptors and enzymes of the arachidonic acid pathway as additional targets with only moderate potencies and efficacies. Finally, a first pharmacokinetic evaluation of archazolid B demonstrated very high degrees of plasma protein binding and rapid degradation of this complex macrolide natural product in mouse, rat and human liver microsomes. The very low pharmacokinetic stability together with the discovery of novel molecular targets which are potently blocked by the archazolids may lead to a reinterpretation of some of the biological data previously discussed for the archazolids and will be of high relevance for the further optimization of the potent anticancer activity of the

archazolids and their advancement as drugs. Our results clearly demonstrate that more stable archazolid analogs are urgently required. Many other archazologs can now be envisioned, which are much more readily accessible, potentially resolving the supply issue and enabling the further development of this promising novel class of potent anticancer drugs. After further addressing the stability issue, these archazologs will be highly useful as synthetically easily accessible simplified macrocyclic compounds allowing comprehensive *in vivo* anticancer studies.

## EXPERIMENTAL SECTION

**General Procedures.** All reagents were purchased from commercial suppliers (Sigma-Aldrich, TCI, Acros, AlfaAesar) in the highest purity grade available and used without further purification. Archazolid A (**1**) and B (**2**) were isolated from mycxobacteria and obtained by common extraction methods.[9a,14c] Bafilomycin A1 (**21**) was purchased from Sigma Aldrich (now Merck). Anhydrous solvents (DCM, $Et_2O$, THF, DCM and toluene) were obtained from a solvent drying system MB SPS-800 (MBrain) and stored over molecular sieves (4 Å). The reactions in which dry solvents were used were performed under an argon atmosphere in flame-dried glassware which had been flushed with argon unless stated otherwise. The reagents were handled using standard Schlenk techniques. TLC monitoring was performed with silica gel 60 $F_{254}$ pre-coated polyester sheets (0.2 mm silica gel, Machery-Nagel) and visualized using UV light and staining with a solution of CAM (1.0 g $Ce(SO_4)_2$), 2.5 g $(NH_4)_6Mo_7O_{24}$, 8 mL conc. $H_2SO_4$ in 100 mL $H_2O$) and subsequent heating.

Semi-preparative and analytical HPLC analyses were performed on *Knauer Wissenschaftliche Geräte GmbH* systems. The solvents for HPLC were purchased in HPLC grade. The products

were detected by their UV absorption at 230 nm or 254 nm, respectively (for further information see SI Section).

The purities of the final products were determined by ESI-mass spectra obtained on an LCMS instrument (Applied Biosystems API 2000 LCMS/MS, HPLC Agilent 1100) using the following procedure: the compounds were dissolved at a concentration of 1.0 mg/mL in acetonitrile containing 2 mM ammonium acetate. Then, 10 $\mu$L of the sample were injected into an HPLC column (Macherey-Nagel Nucleodur® 3 $\mu$ C18, 50 x 2.00 mm). Elution was performed with a gradient of water/acetonitrile (containing 2 mM ammonium acetate) from 90:10 to 0:100 for 20 min at a flow rate of 300 $\mu$L/min, starting the gradient after 10 min. UV absorption was detected from 200 to 950 nm using a diode array detector (DAD). Purity of all compounds was determined at 254 nm. All compounds showed a purity of at least 95% unless otherwise noted.

All NMR spectra were recorded on Bruker spectrometers with operating frequencies of 125, 150, 500, 600 and 700 MHz in deuterated solvents obtained from Deutero. Spectra were measured at room temperature unless stated otherwise and chemical shifts are reported in ppm relative to $(Me)_4Si$ and were calibrated to the residual signal of undeuterated solvents.[29] For full assignment of the $^1$H- and $^{13}$C-NMR signals of the final products: see SI section. Optical rotations were measured with a Perkin Elmar 341 polarimeter in 10 mm cuvette and are uncorrected. High-resolution-mass spectra (HRMS) were recorded on Thermo LTQ Orbitrab Velos mass spectrometer.

**Synthesis of Archazolid F (3) by isomerization.**

To a solution of archazolid B (**2**) (5.0 mg, 6.9 µmol, 1 eq) in dry THF (5 mL) at room temperature DBU (10.5 mg, 69.0 µmol, 10 eq) was added. The resulting solution was stirred at room temperature for 20 h before it was quenched by addition of a saturated solution of $NH_4Cl$

(10 mL) and ethyl acetate (20 mL). The organic phase was separated and the aqueous phase was extracted with ethyl acetate (2 × 25 mL). The combined organic layers were washed with water (30 mL), dried over $MgSO_4$, filtered and concentrated *in vacuo*. Purification of the obtained crude product was performed by HPLC (see SI section) to give archazolid F (**3**) (4.5 mg, 6.2 µmol, 90 %) as a colorless powder together with the recovered starting material archazolid B (0.4 mg, 0.6 µmol, 8 %).

$R_f$ = 0.48 (petrolether/EtOAC = 1/1); $[\alpha]_D^{20}$ = -58° (c 0.1, MeOH); $\lambda_{max}$ = 234 nm; $^1$H-NMR (600 MHz, $CD_3OD$): δ = 7.26 (s, 1H), 6.52 (d, *J* = 15.9 Hz, 1H), 6.18 (dd, *J* = 15.3, 9.9 Hz, 1H), 6.17 (d, *J* = 15.3 Hz, 1H), 5.99 (dd, *J* = 9.3, 4.5 Hz, 1H), 5.81 (d, *J* = 6.4 Hz, 1H), 5.79 (dd, *J* = 16.4, 8.0 Hz, 1H), 5.78 (d, *J* = 10.2 Hz, 1H), 5.78 (dt, *J* = 15.4, 7.2 Hz, 1H), 5.73 (s, 1H), 5.55 (dd, *J* = 15.3, 7.2 Hz, 1H), 5.29 (d, *J* = 9.1 Hz, 1H), 5.22 (d, *J* = 9.8 Hz, 1H), 4.24 (brs, 1 H), 4.09 (dd, *J* = 9.9, 9.9 Hz, 1H), 3.14 (d, *J* = 7.5 Hz, 2H), 3.11 (s, 3H), 3.01 (ddq, *J* = 6.8, 6.8, 6.8 Hz, 1H), 2.71 (s, 3H), 2.32 (ddq, *J* = 9.5, 9.4, 6.7 Hz, 1H), 1.91 (d, *J* = 1.3 Hz, 3H), 1.88 (m, 1H), 1.83 (d, *J* = 0.5 Hz, 3H), 1.78 (s, 3H), 1.78 (m, 1H), 1.75 (m, 1H), 1.73 (m, 1H), 1.59 (s, 3H), 1.03 (d, *J* = 6.9 Hz, 3H), 0.99 (d, *J* = 6.8 Hz, 3H), 0.98 (d, *J* = 6.9 Hz, 3H), 0.83 (d, *J* = 6.7 Hz, 3H), 0.69 (d, *J* = 7.1 Hz, 3H); $^{13}$C-NMR (151 MHz, $CD_3OD$): δ = 174.2, 172.4, 158.2, 155.5, 139.7, 136.5, 135.8, 135.3, 134.9, 134.7, 133.5, 133.2, 132.3, 130.7, 130.0, 129.3, 127.4, 121.9, 117.7, 90.0, 77.4, 76.1, 73.4, 73.3, 56.1, 46.0, 43.9, 41.6 (2x), 39.7, 27.5, 25.8, 24.9, 23.4, 22.3, 20.3, 18.0, 17.3, 13.5, 13.0, 12.4; HRMS (ESI$^+$, 8.0 V): $C_{41}H_{60}N_2O_7SNa$ $[M+Na]^+$: 747.4013 found 747.4008.

**Synthesis of *iso*-Archazolid $A_1$ (4) and $A_2$ (5).**

To a solution of archazolid A (**1**) (5.0 mg, 6.8 µmol, 1 eq) in dry THF (2.5 mL) DBU (10.4 mg, 68.0 µmol, 10 eq) was added. The reaction was stirred at room temperature for 40 h and the

reaction was quenched by addition of saturated $NH_4Cl$ solution (10 mL) and ethyl acetate (20 mL).The organic phase was separated and the aqueous phase was extracted with ethyl acetate (2 × 20 mL). The combined organic layers were washed with water (30 mL), dried over $MgSO_4$, filtered and concentrated *in vacuo*. Purification of the obtained crude product (7.7 mg) was performed by HPLC (see SI section) to give *iso*-archazolid $A_1$ (**4**) (1.1 mg, 1.5 µmol, 22 %), *iso*-archazolid $A_2$ (**5**) (2.3 mg, 3.1 µmol, 46 %) as two colorless powders in a diastereomeric ratio of 1:2.1 together with the recovered starting material archazolid A (0.7 mg, 0.9 µmol, 13 %).

***iso*-Archazolid $A_1$ (4)**

$R_f$ = 0.31 (petrolether/EtAC 1:1); $[\alpha]_D^{20}$ = −81 (c=0.11, MeOH); λ max = 235 nm; $^1$H-NMR (500 MHz, $CD_3OD$): δ [ppm] = 7.27(s, 1H), 6.40 (d, *J* = 15.9 Hz, 1H), 6.23 (d, *J* = 15.4 Hz, 1H), 6.10 (dd, *J* = 15.2, 10.7 Hz, 1H), 5.99 (dd, *J* = 9.1, 4.6 Hz, 1H), 5.81 (dd, *J* = 15.9, 7.8 Hz, 1H), 5.79 (d, *J* = 5.8 Hz, 1H), 5.74 (s, 1H), 5.73 (d, *J* = 9.8 Hz, 1H), 5.67 (dd, *J* = 15.4, 8.8 Hz, 1H), 5.48 (dd, *J* = 15.2, 7.9 Hz, 1H), 5.29 (d, *J* = 9.3 Hz, 1H), 5.18 (dt, *J* = 9.9, 1.4 Hz, 1H), 4.11 (m, 1H), 4.08 (dd, *J* = 9.3, 9.3 Hz, 1H), 3.27 (m, 1H) 3.20 (d, *J* = 9.8Hz, 1H), 3.09 (s, 3H), 2.99 (ddq, *J* = 7.2, 7.2, 6.8 Hz, 1H), 2.71 (s, 3H), 2.30 (ddq, *J* = 9.6, 9.6, 6.7 Hz, 1H), 1.92 (d, *J* = 1.4 Hz, 3H), 1.89 (m, 1H), 1.82 (d, *J* = 1.2 Hz, 3H), 1.79 (m, 1H), 1.78 (s, 3H), 1.75 (m, 1H), 1.73 (m, 1H), 1.57 (d, *J* = 1.3 Hz, 3H), 1.20 (d, *J* = 6.9 Hz, 3H), 1.00 (d, *J* = 6.8 Hz, 3H), 0.99 (d, *J* = 6.0 Hz, 3H), 0.98 (d, *J* = 6.4 Hz, 3H), 0.86 (d, *J* = 6.7 Hz, 3H), 0.71 (d, *J* = 7.0 Hz, 3H); $^{13}$C{$^1$H}-NMR (126 MHz, $CD_3OD$): δ [ppm] = 175.6, 173.9, 158.2, 155.7, 137.7, 136.3, 135.9, 135.4, 135.2, 134.9, 133.6, 133.2, 132.0, 131.1, 129.9, 129.5, 129.1, 127.7, 117.5, 90.0, 77.4, 73.4, 73.3, 56.0, 46.0, 44.8, 44.4, 42.4, 41.7, 27.5, 25.8, 24.9, 23.3, 22.3, 20.2, 17.9 (2×), 17.6, 13.6, 13.5, 12.7; HRMS (ESI$^+$): $C_{42}H_{62}N_2O_7SNa$ $[M+Na]^+$: 761.4170 found 761.4168.

***iso*-Archazolid $A_2$ (5)**

$R_f$ = 0.37 (petrolether/EtOAC = 1/1); $[\alpha]_D^{20}$ = -59° (c=0.1, MeOH); $\lambda_{max}$ = 235 nm; $^1$H-NMR (500 MHz, $CD_3OD$): δ [ppm] = 7.02 (s, 1H), 6.75 (d, *J* = 16.2 Hz, 1H), 6.25 (dd, *J* = 15.0, 11.1 Hz, 1H), 6.17 (d, *J* = 15.5 Hz, 1H), 5.98 (dd, *J* = 9.2, 4.5 Hz, 1H), 5.81 (d, *J* = 4.1 Hz, 1H), 5.79 (d, *J* = 10.9 Hz, 1H), 5.74 (dd, *J* = 16.1, 4.2 Hz, 1H), 5.68 (s, 1H), 5.64 (dd, *J* = 15.5, 8.3 Hz, 1H), 5.50 (dd, *J* = 15.3, 5.3 Hz, 1H), 5.36 (d, *J* = 8.9 Hz, 1H), 5.30 (d, *J* = 9.5 Hz, 1H), 4.46 (brs, 1H), 4.11 (dd, *J* = 9.4, 9.4 Hz, 1H), 3.50 (d, *J* = 9.1Hz, 1H), 3.27 (m, 1H), 3.16 (s, 3H), 3.02 (dt, *J* = 6.4, 4.9 Hz, 1H), 2.71 (s, 3H), 2.36 (ddq, *J* = 9.3, 9.3, 7.3 Hz, 1H), 1.90 (s, 3H), 1.87 (m, 1H), 1.83 (s, 3H), 1.80 (m, 1H), 1.76 (s, 3H), 1.75 (m, 1H), 1.74 (m, 1H), 1.63 (s, 3H), 1.22 (d, *J* = 6.9 Hz, 3H), 1.18 (d, *J* = 6.9 Hz, 3H), 0.99 (d, *J* = 4.9 Hz, 3H), 0.98 (d, *J* = 4.8 Hz, 3H), 0.73 (d, *J* = 6.8 Hz, 3H), 0.66 (d, *J* = 7.2 Hz, 3H); $^{13}C\{^1H\}$-NMR (126 MHz, $CD_3OD$): δ [ppm] = 175.1, 174.0, 158.3, 156.1, 138.3, 136.5, 135.8, 135.2, 134.8, 134.0, 133.5, 133.1, 133.0, 130.8, 130.1, 129.1, 128.5, 126.7, 116.0, 90.0, 77.9, 75.7, 73.5, 73.3, 56.4, 45.9, 44.6, 43.1, 41.3, 40.4, 27.5, 25.8, 24.9, 23.4, 22.3, 20.1, 17.9, 16.6, 16.3, 13.2, 12.5, 11.6; HRMS ($ESI^+$): $C_{42}H_{62}N_2O_7SNa$ $[M+Na]^+$: 761.4170 found 761.4164.

**Synthesis of desmethyl archazolid F (6)**

**Aldehyde 9**

A solution of literature known alcohol **10**[17] (0.10 g, 0.32 mmol, 1.00 eq) in DCM (10 mL) at −78°C was prepared and 2,6-lutidine (48.0 mg, 0.45 mmol, 1.40 eq) and $Et_3SiOTf$ (94.0 µL, 0.42 mmol, 1.30 eq) was added subsequently at this temperature. The reaction was stirred for 45 minutes at −78°C. The reaction was quenched with saturated $NaHCO_3$ (5 mL) solution. After separation of the organic phase, the aqueous phase was extracted with DCM (3×5 mL). The combined organic layers were washed with brine (15 mL) and dried over $MgSO_4$, filtered through a short plug of silica gel (2 cm) and concentrated *in vacuo*.

The residue was solved in toluene (2.5 mL) and acrolein (79.5 µL, 0.96 mmol, 3.00 eq) was added. The solution was refluxed for 30 minutes before Hoveyda-Grubbs catalyst 2nd generation (20.1 mg, 32.0 µmol, 10 mol%) was added. The reaction was refluxed for 20 h. Then the solvent was concentrated *in vacuo*. Purification by column chromatography ($SiO_2$, CyHex/EtAc 10:1 to 4:1) gave aldehyde **9** as an orange oil (42.4 mg, 93.2 µmol, 29%, (20*E*)/(20*Z*): >20/1).

$R_f$ = 0.28 (CyHex/EtAc 4:1); $[\alpha]_D^{20}$ = −65.7 (c=0.21, DCM); $^1$H-NMR (700 MHz, $CD_2Cl_2$): δ [ppm] = 9.45 (d, *J* = 7.9 Hz, 1H), 7.11 (s, 1H), 6.92 (dd, *J* = 7.6, 15.7 Hz, 1H), 5.98 (d, *J* = 8.4 Hz, 1H), 5.97 (dd, *J* = 7.3, 15.7 Hz, 1H), 4.86 (d, *J* = 5.0 Hz, 1H), 4.80 (brs, 1H), 2.98 (ddq, *J* = 6.9, 7.3, 8.4 Hz, 1H), 2.77 (d, *J* = 4.6 Hz, 3H), 1.86 (m, 1H), 1.79 (m, 1H), 1.69 (m, 1H), 1.07 (d, *J* = 6.9 Hz, 3H), 0.94 (m, 6H), 0.89 (t, *J* = 7.9 Hz, 9H), 0.57 (q, *J* = 8.0 Hz, 6H); $^{13}$C{$^1$H}-NMR (176 MHz, $CD_2Cl_2$): δ [ppm] = 194.5, 171.4, 160.7, 159.2, 156.4, 133.3, 115.5, 75.6, 72.4, 44.9, 44.4, 28.0, 25.1, 23.3, 22.5, 16.2, 7.1 (3×), 5.3 (3×); HRMS (ESI-TOF) m/z: $[M+H]^+$ Calcd for $C_{22}H_{38}N_2O_4SSiH^+$ 455.2394, found 455.2406; m/z: $[M+Na]^+$ Calcd for $C_{22}H_{38}N_2O_4SSiNa^+$ 477.2214, found 477.2228.

**Ketone 12**

Preparation of $Ph_2NLi$: Diphenylamine (82.4 mg, 0.48 mmol, 1.00 eq) was dried under high vacuum for 30 minutes. After solving in THF (1.2 mL) *n*-BuLi (0.30 mL, 1.6m in hexane, 0.48 mmol, 1.00 eq) was added at −78°C. The reaction was stirred for 15 minutes at this temperature and additional 15 minutes at 0°C. The reaction results in a 0.32M solution of $Ph_2NLi$ in THF/hexane. The slightly yellow solution was used directly and is highly sensitive against oxidation (green solution).

Ketone **11**[17d] (40.0 mg, 69.6 µmol, 1.00 eq) was dried by azeotropic evaporation with toluene (2×5 mL) and then solved in THF (1 mL). At −78°C $Ph_2NLi$ (375 µL, 0.32M in THF/hexane,

0.12 mmol, 1.75 eq) was added. The reaction was stirred for 30 minutes at this temperature and additional 30 minutes at −40°C. Then aldehyde **9** (41.1 mg, 90.4 µmol, 1.30 eq, in 0.3 mL THF) was added dropwise at −78°C. The reaction was stirred at this temperature for 1 h. Then the reaction was quenched with saturated $NaHCO_3$ solution (5 mL) and was diluted with $Et_2O$ (5 mL) at 0°C. After separation of the organic phase, the aqueous phase was extracted with $Et_2O$ (3×5 mL). The combined organic layers were washed with brine (15 mL), dried over $MgSO_4$ and concentrated *in vacuo*. Purification by column chromatography ($SiO_2$ , CyHex/EtAc 10:1 to 5:1) gave the aldol product which is directly converted in the acetate by dissolving it in THF (2 mL). It was dried over 3Å MS for 30 minutes. Then DMAP (84.2 mg, 0.69 mmol, 10.0 eq) and $Ac_2O$ (58.7 µL, 0.62 mmol, 9.00 eq) was added at 0°C subsequently. The reaction was stirred for 30 minutes at room temperature. After addition of DBU (0.36 mL, 2.41 mmol, 35.0 eq) the reaction was stirred over night. After 17 h the reaction was quenched with saturated $NaHCO_3$ solution (5 mL) and was diluted with $Et_2O$ (5 mL) at 0°C. After separation of the organic phase, the aqueous phase was extracted with $Et_2O$ (3×5 mL). The combined organic layers were washed with brine (15 mL), dried over $MgSO_4$ and concentrated in vacuo. Purification by column chromatography ($SiO_2$ , CyHex/EtAc 8:1) gave the unsaturated ketone **12** as an orange oil (27.9 mg, 27.6 µmol, 40% over 3 steps, (18*E*) as single conformer.)

$R_f$ = 0.45 (CyHex/EtAc 5:1); $[\alpha]_D^{20}$ = −45.0 (c=0.18, DCM); $^1$H-NMR (700 MHz, $CD_2Cl_2$): δ [ppm] = 7.07 (s, 1H), 6.96 (d, *J* = 10.8 Hz, 1H), 6.36 (ddd, *J* = 0.6, 10.8, 17.4 Hz, 1H), 6.32 (d, *J* = 15.8 Hz, 1H), 6.29 (dd, *J* = 11.0, 15.2 Hz, 1H), 6.10 (dd, *J* = 8.5, 15.1 Hz, 1H), 5.98 (dd, *J* = 5.3, 8.6 Hz, 1H), 5.87 (s, 1H), 5.53 (dd, *J* = 7.6, 15.8 Hz, 1H), 5.39 (d, *J* = 9.0 Hz, 1H), 5.14 (d, *J* = 17.4 Hz, 1H), 5.09 (dt, *J* = 1.4, 9.7 Hz, 1H), 4.99 (d, *J* = 10.8 Hz, 1H), 4.79 (d, *J* = 4.8 Hz, 1H), 4.78 (brs, 1H), 4.25 (dd, *J* = 5.6, 9.0 Hz, 1H), 4.22 (dd, *J* = 7.2, 7.2 Hz, 1H), 3.42 (dq, *J* = 6.9,

7.0 Hz, 1H), 2.82 (ddq, *J* = 4.8, 6.8, 7.4 Hz, 1H), 2.77 (d, *J* = 4.9 Hz, 3H), 2.39 (ddq, *J* = 5.6, 6.8, 9.7 Hz, 1H), 1.87 (m, 1H), 1.80 (m, 1H), 1.76 (m, 6H), 1.72 (s, 3H), 1.71 (d, *J* = 1.2 Hz, 3H), 1.70 (m, 1H), 1.08 (d, *J* = 6.7 Hz, 3H), 1.04 (d, *J* = 6.9 Hz, 3H), 0.95 (m, 6H), 0.88 (t, *J* = 8.0 Hz, 9H), 0.88 (d, *J* = 6.7 Hz, 3H), 0.87 (s, 9H), 0.85 (s, 9H), 0.56 (q, *J* = 8.0 Hz, 6H), 0.02 (s, 3H), 0.00 (s, 3H), -0.03 (s, 3H), -0.05 (s, 3H); $^{13}C\{^{1}H\}$-NMR (176 MHz, $CD_2Cl_2$): δ [ppm] = 204.2, 171.0, 159.9, 156.4, 145.4, 142.1, 139.1, 135.5, 135.4, 133.9, 133.2, 133.0, 132.5, 132.2, 130.4, 129.6, 127.6, 115.2, 112.2, 77.3, 76.1, 73.3, 72.5, 60.8, 46.8, 45.2, 45.0, 41.1, 28.0, 26.2 (3×), 26.1 (3×), 25.2, 23.3, 22.5, 20.6, 18.60, 18.58, 17.4, 16.1, 14.8, 12.8, 12.0, 7.1 (3×), 5.3 (3×), −3.7, −4.2, −4.5, −4.6; HRMS (ESI-TOF) m/z: $[M+Na]^+$ Calcd for $C_{56}H_{98}N_2O_6SSi_3Na^+$ 1033.6346, found 1033.6338.

**Alcohol 13**

Preparation of HF×pyridine stock solution: At 0°C was added subsequently pyridine (375 µL) and HF×pyridine (70% HF, 125 µL) to THF (0.65 mL).

Preparation of activated acid stock solution: At 0°C was added DCC (0.29 mL, 1m in DCM, 0.29 mmol, 1.00 eq) to a solution of vinylacetic acid (25.0 µL, 0.29 mmol, 1.03 eq) in DCM (435 µL). This results in a 0.4M solution of activated acid in DCM. The solution was used immediately within seconds.

To a solution of TES protected alcohol **12** (15.0 mg, 14.8 µmol, 1.00 eq) in THF (0.5 mL) at 0°C was added HF×pyridine stock solution (0.6 mL). The reaction was stirred for 45 minutes at 0°C. The reaction was quenched at 0°C with pH 7 buffer solution (3 mL) and diluted with EtAc (3 mL). After separation of the organic phase, the aqueous phase was extracted with EtAc (2×3 mL). The combined organic layers were washed with a mixture of brine and saturated $NaHCO_3$ solution (1:1, 3 mL) which was afterwards extracted with EtAc (1×3 mL). The combined organic

layers were dried over $MgSO_4$ and concentrated *in vacuo*. The residue was solved in DCM (0.10 mL) and activated acid stock solution (0.15 mL, 0.4M in DCM, 60.0 µmol, 4.05 eq) was added at 0°C before DMAP (0.4 mg, 2.97 µmol, 20 mol%) was added. The reaction was stirred for 25 minutes at 0°C. The reaction was quenched at 0°C with half saturated $NH_4Cl$ solution (2 mL) and diluted with EtAc (3 mL). After separation of the organic phase, the aqueous phase was extracted with EtAc (2×3 mL). The combined organic layers were washed with brine (3 mL) which was afterwards extracted with EtAc (1×3 mL). The combined organic layers were dried over $MgSO_4$ and concentrated *in vacuo*. Purification by column chromatography ($SiO_2$, CyHex/EtAc 7:1) gave vinylacetyl ester which was directly solved in MeOH (0.5 mL). At 0°C $NaBH_4$ (2.2 mg, 59.2 µmol, 4.00 eq) was added. The reaction was stirred for 1 h at 0°C. Then another portion of $NaBH_4$ (2.2 mg, 59.2 µmol, 4.00 eq) was added. After 15 minutes stirring at 0°C the reaction was diluted with EtAc (2 mL) and quenched with half saturated $NH_4Cl$ solution (2 mL). After separation of the organic phase, the aqueous phase was extracted with EtAc (3×2 mL). The combined organic layers were washed with brine (2 mL), dried over $MgSO_4$ and concentrated in vacuo. Purification by column chromatography ($SiO_2$, CyHex/EtAc 4:1) gave the alcohol **13** as a colourless oil (9.4 mg, 9.7 µmol, 66% over 2 steps, *dr* 5:1).

$R_f$ = 0.40 (CyHex/EtAc 5:1); $[\alpha]_D^{20}$ = +10.0 (c=0.27, DCM); $^1$H-NMR (700 MHz, $CD_2Cl_2$): δ [ppm] = 7.11 (s, 1H), 6.45 (d, *J* = 15.8 Hz, 1H), 6.36 (ddd, *J* = 0.8, 10.8, 17.4 Hz, 1H), 6.23 (dd, *J* = 10.8, 15.0 Hz, 1H), 5.99 (dd, *J* = 5.5, 9.1 Hz, 1H), 5.89 (m, 3H), 5.77 (dd, *J* = 8.0, 15.2 Hz, 1H), 5.77 (d, *J* = 6.9 Hz, 1H), 5.53 (dd, *J* = 8.5, 15.1 Hz, 1H), 5.39 (d, *J* = 8.9 Hz, 1H), 5.14 (m, 3H), 5.08 (dt, *J* = 1.3, 9.7 Hz, 1H), 4.99 (d, *J* = 10.8 Hz, 1H), 4.83 (m, 1H), 4.42 (dd, *J* = 2.1, 7.6 Hz, 1H), 4.26 (dd, *J* = 5.7, 9.0 Hz, 1H), 3.88 (d, *J* = 2.0, 9.3 Hz, 1H), 3.79 (d, *J* = 2.0 Hz, 1H), 3.10 (ddt, *J* = 1.4, 2.9, 6.9 Hz, 2H), 2.98 (m, 1H), 2.77 (d, *J* = 4.8 Hz, 3H), 2.43 (ddq, *J* =

5.7, 6.7, 9.1 Hz, 1H), 1.88 (d, *J* = 1.3 Hz, 3H), 1.86 (m, 2H), 1.81 (m, 2H), 1.78 (s, 3H), 1.71 (d, *J* = 1.2 Hz, 3H), 1.66 (d, *J* = 0.4 Hz, 3H), 0.96 (d, *J* = 6.7 Hz, 3H), 0.96 (d, *J* = 6.7 Hz, 3H), 0.95 (d, *J* = 7.1 Hz, 3H), 0.91 (s, 9H), 0.86 (d, *J* = 7.0 Hz, 3H), 0.85 (s, 9H), 0.63 (d, *J* = 7.0 Hz, 3H), 0.09 (s, 3H), 0.04 (s, 3H), 0.00 (s, 3H), −0.04 (s, 3H); $^{13}C\{^{1}H\}$-NMR (176 MHz, $CD_2Cl_2$): δ [ppm] = 173.1, 171.1, 156.4, 154.6, 142.0, 138.3, 135.2, 134.8, 133.9, 133.2, 132.9, 132.4, 131.0, 130.73, 130.72, 130.1, 128.0, 127.4, 118.8, 118.2, 112.2, 81.0, 78.3, 76.0, 73.2, 72.5, 45.0, 42.4, 42.0, 41.0, 39.7, 31.5, 26.2 (3×), 26.1 (3×), 25.2, 25.0, 23.3, 22.4, 20.7, 18.6, 18.5, 17.3, 15.8, 14.4, 12.8, 11.6, -3.8, −4.2, −4.7, −4.8; HRMS (ESI-TOF) m/z: $[M+Na]^+$ Calcd for $C_{54}H_{90}N_2O_7SSi_2Na^+$ 989.5899, found 989.5909.

**Desmethylarchazolid F (6)**

A solution of ester **13** (9.0 mg, 9.30 µmol, 1.00 eq) in toluene (12.4 mL resulting in a 0.75 mM solution) was refluxed for 30 minutes. Then metathese catalyst **14** (0.72 mg, 0.93 µmol, 10 mol%) was added in toluene (0.5 mL). The solution was refluxed for 2 h and afterwards another portion of metathese catalyst **14** (0.72 mg, 0.93 µmol, 10 mol%) was added in toluene (0.5 mL). The solution was refluxed for additional 2 h. Then the reaction was concentrated *in vacuo*. Purification by column chromatography ($SiO_2$, CyHex/EtAc 3:1) gave a mixture of starting material, TBS-protected desmethyl archazolid F (major) and minor stereoisomers (7.5 mg). The ring closing was controlled by COSY NMR.

For deprotection, the mixture was solved in THF (0.5 mL) and at 0°C pyridine (0.3 mL) and HF×pyridine (70%, 0.2 mL) was added subsequently. The reaction was stirred for 5.5 h at room temperature. Then the reaction was quenched at 0°C with pH 7 buffer solution (3 mL) and diluted with EtAc (3 mL). After separation of the organic phase, the aqueous phase was extracted with EtAc (3×2 mL). The combined organic layers were washed with a saturated $NaHCO_3$

solution (3 mL) and brine (3 mL). Both aqueous phases were extracted with EtAc (1×3 mL). The combined organic layers were dried over $MgSO_4$ and concentrated *in vacuo*. Purification by column chromatography (SiO 2 , CyHex/EtAc 1:1) gave a mixture of products (3.4 mg) which were further purified by HPLC (see SI Section). Desmethyl archazolid F (**6**) was obtained as a white solid (1.6 mg, 2.25 µmol, 24% over 2 steps).

$R_f$ = 0.42 (CyHex/EtAc 2:3); $[\alpha]_D^{20}$ = +130.0 (c=0.04, DCM); $^1$H-NMR (700 MHz, $CD_2Cl_2$): δ [ppm] = 7.14 (s, 1H), 6.63 (dd, *J* = 1.5, 15.9 Hz, 1H), 6.26 (dd, *J* = 10.8, 15.1 Hz, 1H), 6.09 (d, *J* = 15.9 Hz, 1H), 6.00 (dd, *J* = 5.0, 9.2 Hz, 1H), 5.92 (dd, *J* = 3.6, 15.9 Hz, 1H), 5.80 (d, *J* = 10.6 Hz, 1H), 5.77 (s, 1H), 5.73 (d, *J* = 9.3 Hz, 1H), 5.69 (ddd, *J* = 4.9, 7.4, 16.0 Hz, 1H), 5.54 (dd, *J* = 9.4, 15.0 Hz, 1H), 5.27 (dt, *J* = 1.3, 9.6, 1H), 5.24 (d, *J* = 8.8 Hz, 1H), 4.83 (brs, 1H), 4.83 (brs, 1H), 4.68 (brs, 1H), 4.36 (brs, 1H), 4.10 (dd, *J* = 9.6, 9.6 Hz, 1H), 3.88 (dd, *J* = 3.0, 10.2 Hz, 1H), 3.07 (ddd, *J* = 1.8, 4.9, 16.0 Hz, 1H), 3.01 (ddd, *J* = 1.1, 7.5, 15.8 Hz, 1H), 3.01 (m, 1H), 2.78 (d, *J* = 4.8, 3H), 2.43 (s, 1H), 2.32 (ddq, *J* = 6.8, 6.8, 9.8 Hz, 1H), 2.15 (ddq, *J* = 3.7, 7.4, 11.1 Hz, 1H), 1.92 (d, *J* = 1.3 Hz, 3H), 1.89 (m, 1H), 1.83 (s, 3H), 1.80 (m, 1H), 1.76 (d, *J* = 1.1 Hz, 3H), 1.71 (m, 1H), 1.67 (d, *J* = 1.1 Hz, 3H), 0.97 (d, *J* = 6.5 Hz, 3H), 0.96 (d, *J* = 6.6 Hz, 3H), 0.86 (d, *J* = 6.7, 3H), 0.79 (d, *J* = 6.8 Hz, 3H), 0.67 (d, *J* = 7.3 Hz, 3H); $^{13}$C{$^1$H}-NMR (176 MHz, $CD_2Cl_2$): δ [ppm] = 172.5, 171.0, 156.4, 154.3, 138.2, 137.9, 137.8, 137.6, 136.1, 133.5, 132.1, 131.3, 130.6, 128.7, 128.2, 127.6, 127.3, 121.6, 118.0, 81.2, 76.8, 75.7, 73.4, 72.8, 45.1, 42.7, 41.4, 40.1, 37.8, 28.0, 25.2, 25.0, 23.3, 22.4, 20.5, 18.3, 17.2, 14.8, 13.6, 11.1; HRMS (ESI-TOF) m/z: $[M+Na]^+$ Calcd for $C_{40}H_{58}N_2O_7SNa^+$ 733.3857, found 733.3842.

**Synthesis of archazolog (7)**

**Aldehyde 17**

At −78°C dimethyl glutaconate (**16**) (2.00 mL, 14.2 mmol, 1.00 eq) was stirred in DCM (400 mL) and DIBALH (77.5 mL, 1.1M in hexane, 85.2 mmol, 6.00 eq) was added. The reaction was stirred for 1.5 h at −78°C. Then the reaction was warmed to 0°C and stirred for additional 45 minutes. Then the reaction was diluted with $Et_2O$ (250 mL) and quenched with $H_2O$ (3.40 mL), 3M NaOH (3.40 mL) and additional $H_2O$ (8.00 mL). After stirring for 30 minutes at room temperature the reaction was dried over $MgSO_4$ and concentrated in vacuo. The residue was solved in DCM (200 mL) and $MnO_2$ (18.5 g, 0.21 mol, 15.0 eq) was added in one portion. The reaction was stirred over night. The reaction was filtered and concentrated *in vacuo*. Purification by column chromatography ($SiO_2$, EtAc) gave aldehyde **17** as a colourless oil (0.61 g, 5.99 mmol, 42%).

$R_f$ = 0.29 (EtAc); $^1$H-NMR (500 MHz, $CD_2Cl_2$): δ [ppm] = 9.50 (d, *J* = 7.8 Hz, 1H), 6.89 (dt, *J* = 6.9, 15.7 Hz, 1H), 6.16 (ddt, *J* = 1.5, 7.8, 15.7 Hz, 1H), 3.79 (dt, *J* = 6.1, 6.1 Hz, 2H), 2.58 (ddt, *J* = 1.5, 6.1, 6.9 Hz, 2H), 1.66 (t, *J* = 5.0 Hz, 1H); $^{13}$C{$^1$H}-NMR (126 MHz, $CD_2Cl_2$): δ [ppm] = 194.2, 155.5, 135.0, 61.2, 36.4. The spectroscopic data were in agreement with those previously reported.[30]

**Aldehyde 15**

To a solution of alcohol **17** (0.30 g, 3.00 mmol, 1.00 eq) in DCM (30 mL) at −78°C was added 2,6-lutidine (0.52 mL, 4.49 mmol, 1.50 eq) and TBSOTf (0.88 mL, 3.90 mmol, 1.30 eq). The reaction was stirred for 60 minutes at this temperature. Afterwards the reaction was quenched at −78°C with saturated $NaHCO_3$ solution (30 mL) and allowed to warm up to room temperature. After separation of the organic phase, the aqueous phase was extracted with DCM (2×30 mL). The combined organic layers were dried over $MgSO_4$ and concentrated in vacuo. Purification by

column chromatography ($SiO_2$, CyHex/EtAc 10:1) gave silylether **15** as a colourless liquid (0.32 g, 1.49 mmol, 50%).

$R_f$ = 0.28 (CyHex/EtAc 10:1); $^1$H-NMR (500 MHz, $CD_2Cl_2$): δ [ppm] = 9.49 (d, *J* = 7.9 Hz, 1H), 6.88 (dt, *J* = 6.9, 15.7 Hz, 1H), 6.13 (ddt, *J* = 1.5, 7.9, 15.7 Hz, 1H), 3.78 (t, *J* = 6.2 Hz, 2H), 2.53 (ddt, *J* = 1.5, 6.2, 6.9 Hz, 2H), 0.89 (s, 9H), 0.06 (6H); $^{13}$C{$^1$H}-NMR (126 MHz, $CD_2Cl_2$ ): δ [ppm] = 194.3, 156.2, 134.8, 61.8, 36.7, 26.2 (3×), 18.7, −5.1 (2×); HRMS (ESI-TOF) m/z: $[M+Na]^+$ Calcd for $C_{11}H_{22}O_2SiNa^+$ 237.1281, found 237.1276.

**Unsaturated Ketone (18)**

Preparation of $Ph_2NLi$: Diphenylamine (92.7 mg, 0.55 mmol, 1.00 eq) was dried under high vacuum for 30 minutes. After solving in THF (1.8 mL) *n*-BuLi (0.34 mL, 1.6M in hexane, 0.55 mmol, 1.00 eq) was added at −78°C. The reaction was stirred for 15 minutes at this temperature and additional 15 minutes at 0°C. The reaction results in a 0.26M solution of $Ph_2NLi$ in THF/hexane. The slightly yellow solution was used directly and is highly sensitive against oxidation (green solution).

Ketone **11** (0.15 g, 0.26 mmol, 1.00 eq) was dried by azeotropic evaporation with toluene (2×10 mL) and then solved in THF (2.5 mL). At −78°C $Ph_2NLi$ (1.40 mL, 0.26M in THF/hexane, 0.36 mmol, 1.40 eq) was added. The reaction was stirred for 30 minutes at this temperature and additional 30 minutes at −40°C. Then aldehyde **15** (67.1 mg, 0.31 mmol, 1.20 eq, dried over 3Å MS in 1.0 mL THF) was added dropwise at −78°C. The reaction was stirred at this temperature for 75 minutes. Then the reaction was quenched with saturated $NaHCO_3$ solution (5 mL) and was diluted with $Et_2O$ (5 mL) at 0°C. After separation of the organic phase, the aqueous phase was extracted with $Et_2O$ (3×5 mL). The combined organic layers were washed with saturated $NH_4Cl$ solution (15 mL) and brine (15 mL), dried over $MgSO_4$ and concentrated

*in vacuo*. Purification by column chromatography ($SiO_2$ , CyHex/EtAc 30:1) gave the aldol product which is directly converted in the acetate by dissolving it in THF (15 mL). It was dried over 3Å MS for 30 minutes. Then DMAP (0.31 g, 2.59 mmol, 10.0 eq) and Ac 2 O (0.22 mL, 2.34 mmol, 9.00 eq) was added at 0°C subsequently. The reaction was stirred for 45 minutes at room temperature. After addition of DBU (1.36 mL, 9.09 mmol, 35.0 eq) the reaction was stirred over night. After 17 h the reaction was quenched with saturated $NaHCO_3$ solution (10 mL) and was diluted with $Et_2O$ (5 mL) at 0°C. After separation of the organic phase, the aqueous phase was extracted with $Et_2O$ (3×10 mL). The combined organic layers were washed with brine (20 mL), dried over MgSO 4 and concentrated in vacuo. Purification by column chromatography ($SiO_2$, CyHex/EtAc 30:1) gave the unsaturated ketone **18** as a colourless oil (0.18 g, 0.24 mmol, 92% over 3 steps, (18*E*) as single conformer).

$R_f$ = 0.53 (CyHex/EtAc 20:1); $[\alpha]_D^{20}$ = +3.8 (c=0.24, DCM); $^1$H-NMR (700 MHz, $CD_2Cl_2$): δ [ppm] = 6.99 (d, *J* = 11.1 Hz, 1H), 6.50 (ddt, *J* = 1.4, 10.9, 15.0 Hz, 1H), 6.37 (ddd, *J* = 0.7, 10.7, 17.3 Hz, 1H), 6.33 (d, *J* = 15.6 Hz, 1H), 6.13 (dt, *J* = 14.7, 7.2 Hz, 1H), 5.87 (s, 1H), 5.55 (dd, *J* = 7.7, 15.6 Hz, 1H), 5.39 (d, *J* = 9.0 Hz, 1H), 5.14 (d, *J* = 17.5 Hz, 1H), 5.09 (dt, *J* = 1.4, 9.7 Hz, 1H), 4.99 (d, *J* = 10.8 Hz, 1H), 4.25 (dd, *J* = 5.6, 9.0 Hz, 1H), 4.24 (dd, *J* = 7.1, 7.1 Hz, 1H), 3.71 (t, *J* = 6.4 Hz, 2H), 3.42 (dq, *J* = 6.8, 6.8 Hz, 1H), 2.41 (dt, *J* = 6.5, 6.5 Hz, 2H), 2.38 (ddq, *J* = 5.6, 6.5, 9.7 Hz, 1H), 1.78 (d, *J* = 0.6 Hz, 3H), 1.76 (d, *J* = 1.3 Hz, 6H), 1.71 (d, *J* = 1.2 Hz, 3H), 1.09 (d, *J* = 6.8 Hz, 3H), 0.89 (s, 9H), 0.88 (d, *J* = 6.8 Hz, 3H), 0.87 (s, 9H), 0.85 (s, 9H), 0.06 (s, 6H), 0.02 (s, 3H), 0.00 (s, 3H), -0.02 (s, 3H), -0.05 (s, 3H); $^{13}$C{$^1$H}-NMR (176 MHz, $CD_2Cl_2$): δ [ppm] = 204.2, 142.1, 140.3, 138.7, 135.6, 135.4, 133.9, 133.2, 133.0, 132.4, 132.2, 130.5, 129.7, 128.9, 112.2, 77.3, 73.3, 62.8, 46.9, 41.1, 37.5, 26.23 (3×), 26.19 (3×), 26.14

(3×), 25.1, 20.6, 18.7, 18.60, 18.58, 16.1, 14.7, 12.8, 12.1, −3.7, −4.2, −4.5, −4.6, −5.0 (2×); HRMS (ESI-TOF) m/z: $[M+Na]^+$ Calcd for $C_{45}H_{82}O_4Si_3Na^+$ 793.5413, found 793.5429.

**Methyl ether 19**

A solution of ketone **18** (0.18 g, 0.24 mmol, 1.00 eq) in THF (1 mL) was diluted with MeOH (5 mL). At 0°C $NaBH_4$ (35.9 mg, 0.95 mmol, 4.00 eq) was added and after stirring for 45 minutes additional $NaBH_4$ (35.9 mg, 0.95 mmol, 4.00 eq) was added. After another 30 minutes at 0°C another portion $NaBH_4$ (35.9 mg, 0.95 mmol, 4.00 eq) was added. After 1.5 h the reaction was carefully quenched with saturated $NH_4Cl$ solution (3 mL). After separation of the organic phase, the aqueous phase was extracted with $Et_2O$ (3×5 mL). The combined organic layers were washed with brine (10 mL), dried over $MgSO_4$ and concentrated *in vacuo*. Purification by column chromatography ($SiO_2$, CyHex/EtAc 20:1) gave the corresponding alcohol **22** as a slightly yellow oil (0.17 g, 0.22 mmol, 92%, dr 8.2:1).

$R_f$ = 0.35 (CyHex/EtAc 30:1); $[\alpha]_D^{20}$ = +30.0 (c=0.05, DCM); $^1$H-NMR (500 MHz, $CD_2Cl_2$): δ [ppm] = 6.45 (d, *J* = 15.8 Hz, 1H), 6.36 (dd, *J* = 10.7, 17.4 Hz, 1H), 6.32 (ddt, *J* = 1.3, 10.9, 15.0 Hz, 1H), 5.92 (d, *J* = 10.7 Hz, 1H), 5.90 (s, 1H), 5.78 (dd, *J* = 7.6, 15.8 Hz, 1H), 5.65 (dt, *J* = 7.1, 14.7 Hz, 1H), 5.39 (d, *J* = 8.9 Hz, 1H), 5.14 (d, *J* = 17.5 Hz, 1H), 5.09 (dt, *J* = 1.3, 9.7 Hz, 1H), 4.99 (d, *J* = 10.8 Hz, 1H), 4.43 (dd, *J* = 2.2, 7.6 Hz, 1H), 4.26 (dd, *J* = 5.6, 9.0 Hz, 1H), 3.89 (d, *J* = 8.0 Hz, 1H), 3.79 (d, *J* = 2.0 Hz, 1H), 3.65 (dt, *J* = 1.0, 6.6 Hz, 2H), 2.43 (ddq, *J* = 5.6, 6.7, 9.6 Hz, 1H), 2.31 (dt, *J* = 6.7, 6.7 Hz, 2H), 1.89 (d, *J* = 1.3 Hz, 3H), 1.86 (m, 1H), 1.78 (s, 3H), 1.71 (d, *J* = 1.2 Hz, 3H), 1.69 (s, 3H), 0.91 (s, 9H), 0.89 (s, 9H), 0.87 (d, *J* = 6.9 Hz, 3H), 0.86 (s, 9H), 0.65 (d, *J* = 7.1 Hz, 3H), 0.09 (s, 3H), 0.04 (s, 9H), 0.00 (s, 3H), −0.04 (s, 3H); $^{13}$C{$^1$H}-NMR (126 MHz, $CD_2Cl_2$): δ [ppm] = 142.1, 137.5, 135.2, 133.9, 133.2, 132.9, 132.4, 131.2, 130.7, 130.2, 128.5, 127.6, 112.2, 81.1, 78.3, 73.2, 63.5, 42.4, 41.0, 37.1, 27.5, 26.3 (3×),

26.17 (3×), 26.15 (3×), 25.0, 20.7, 18.8, 18.6, 18.5, 15.8, 13.0, 12.8, 11.6, −3.8, −4.2, −4.6, −4.7, −5.0 (2×); HRMS (ESI-TOF) m/z: $[M+Na]^+$ Calcd for $C_{45}H_{84}O_4Si_3Na^+$ 795.5570, found 795.5555.

To a solution of the above prepared alcohol **22** (29.0 mg, 37.5 µmol, 1.00 eq) and proton sponge (44.2 mg, 0.21 mmol, 5.50 eq) in DCM (2 mL) at 0°C was added $Me_3OBF_4$ (27.7 mg, 0.19 mmol, 5.00 eq). The reaction was stirred for 2 h 45 minutes at 0°C. Afterwards the reaction was quenched at 0°C with saturated $NaHCO_3$ solution (2 mL). After separation of the organic phase, the aqueous phase was extracted with DCM (3×3 mL). The combined organic layers were dried over $MgSO_4$ and concentrated *in vacuo*. Purification by column chromatography ($SiO_2$ , CyHex/EtAc 30:1) gave methyl ether **19** as a colourless oil (26.5 mg, 33.7 µmol, 90%).

$R_f$ = 0.41 (CyHex/EtAc 30:1); $[\alpha]_D^{20}$D = +31.0 (c=0.40, DCM); $^1$H-NMR (700 MHz, $CD_2Cl_2$): δ [ppm] = 6.42 (d, *J* = 15.9 Hz, 1H), 6.36 (ddd, *J* = 0.8, 10.8, 17.4 Hz, 1H), 6.35 (ddt, *J* = 1.4, 10.9, 15.1 Hz, 1H), 5.91 (d, *J* = 10.8 Hz, 1H), 5.84 (s, 1H), 5.72 (dd, *J* = 7.0, 15.7 Hz, 1H), 5.68 (dt, *J* = 7.2, 14.7 Hz, 1H), 5.40 (d, *J* = 9.0 Hz, 1H), 5.14 (d, *J* = 17.7 Hz, 1H), 5.07 (dt, *J* = 1.4, 9.7 Hz, 1H), 4.99 (d, *J* = 10.8 Hz, 1H), 4.69 (dt, *J* = 1.6, 6.9 Hz, 1H), 4.25 (dd, *J* = 5.6, 9.0 Hz, 1H), 3.66 (t, *J* = 6.6 Hz, 2H), 3.34 (d, *J* = 9.9 Hz, 1H), 3.10 (s, 3H), 2.43 (ddq, *J* = 5.6, 6.7, 9.7 Hz, 1H), 2.32 (dt, *J* = 6.6, 6.6 Hz, 2H), 1.84 (d, *J* = 1.3 Hz, 3H), 1.79 (s, 3H), 1.71 (d, *J* = 1.2 Hz, 3H), 1.58 (m, 1H), 1.57 (s, 3H), 0.92 (s, 9H), 0.89 (s, 9H), 0.88 (d, *J* = 6.8 Hz, 3H), 0.85 (s, 9H), 0.63 (d, *J* = 7.0 Hz, 3H), 0.05 (s, 3H), 0.05 (s, 6H), 0.00 (s, 6H), −0.05 (s, 3H); $^{13}$C{$^1$H}-NMR (176 MHz, $CD_2Cl_2$): δ [ppm] = 142.1, 135.2, 134.8, 134.7, 133.9, 133.34, 133.32, 132.4, 131.3, 130.2, 129.5, 128.4, 128.3, 112.1, 88.8, 73.2, 72.3, 63.4, 55.9, 43.3, 41.0, 37.1, 26.3 (3×), 26.2 (3×), 26.1 (3×), 25.1, 20.7, 18.8, 18.7, 18.6, 15.6, 12.8, 10.9, 9.3, −3.5, −4.2, −4.7, −4.8, −5.0 (2×); HRMS (ESI-TOF) m/z: $[M+Na]^+$ Calcd for $C_{46}H_{86}O_4Si_3Na^+$ 809.5726, found 809.5731.

**Ester 20**

Preparation of HF×pyridine stock solution: To a solution of THF (1.3 mL) and pyridine (0.75 mL) was added HF×pyridine (0.25 mL, 70% HF).

To a solution of silylether **19** (0.12 g, 0.15 mmol, 1.00 eq) in THF (1 mL) at 0 ◦ C was added HF×pyridine stock solution (2 mL). The reaction was stirred for 5 h 30 minutes at 0 ◦ C. The reaction was diluted with $H_2O$ (5 mL) and $Et_2O$ (4 mL). After separation of the organic phase, the aqueous phase was extracted with $Et_2O$ (3×5 mL). The combined organic layers were dried over MgSO 4 and concentrated *in vacuo*. Purification by column chromatography (SiO 2 , CyHex/EtAc 5:1) gave alcohol **23** as a colourless oil (84.1 mg, 0.12 mmol, 84%).

$R_f$ = 0.20 (CyHex/EtAc 10:1); $[\alpha]_D^{20}$ = +24.3 (c=0.07, DCM); $^1$H-NMR (700 MHz, $CD_2Cl_2$): δ [ppm] = 6.42 (d, *J* = 15.9 Hz, 1H), 6.40 (ddt, *J* = 1.3, 10.8, 15.0 Hz, 1H), 6.37 (ddd, *J* = 0.7, 10.7, 17.3 Hz, 1H), 5.93 (d, *J* = 10.8 Hz, 1H), 5.84 (s, 1H), 5.72 (dd, *J* = 6.9, 15.9 Hz, 1H), 5.67 (dt, *J* = 7.2, 14.7 Hz, 1H), 5.40 (d, *J* = 9.1 Hz, 1H), 5.14 (d, *J* = 17.4 Hz, 1H), 5.07 (dt, *J* = 1.4, 9.7 Hz, 1H), 4.99 (d, *J* = 10.7 Hz, 1H), 4.69 (d, *J* = 6.9 Hz, 1H), 4.25 (dd, *J* = 5.6, 9.0 Hz, 1H), 3.65 (dt, *J* = 5.8, 6.3 Hz, 2H), 3.35 (d, *J* = 9.9 Hz, 1H), 3.10 (s, 3H), 2.43 (ddq, *J* = 5.6, 6.7, 9.7 Hz, 1H), 2.36 (dt, *J* = 6.3 Hz, 2H), 1.84 (d, *J* = 1.3 Hz, 3H), 1.79 (s, 3H), 1.71 (d, *J* = 1.2 Hz, 3H), 1.60 (m, 1H), 1.58 (s, 3H), 1.40 (t, *J* = 5.8 Hz), 0.92 (s, 9H), 0.88 (d, *J* = 6.8 Hz, 3H), 0.85 (s, 9H), 0.63 (d, *J* = 7.0 Hz, 3H), 0.05 (s, 3H), 0.00 (s, 6H), -0.04 (s, 3H); $^{13}$C{$^1$H}-NMR (176 MHz, $CD_2Cl_2$): δ [ppm] = 142.1, 135.5, 135.2, 134.6, 133.9, 133.33, 133.31, 132.4, 130.7, 129.9, 129.6, 129.1, 128.3, 112.1, 88.7, 73.2, 72.3, 62.5, 56.0, 43.3, 41.0, 37.0, 26.3 (3×), 26.1 (3×), 25.1, 20.7, 18.7, 18.6, 15.6, 12.8, 11.0, 9.4, -3.5, -4.2, -4.7, -4.8.

Preparation of activated acid stock solution: At 0°C was added DCC (0.36 mL, 1M in DCM, 0.36 mmol, 1.00 eq) to a solution of vinylacetic acid (32.0 µL, 0.38 mmol, 1.05 eq) in DCM

(4.11 mL). This results in a 0.08M solution of activated acid in DCM. The solution was used immediately within seconds.

To a solution of alcohol **23** (84.1 mg, 0.12 mmol, 1.00 eq) in DCM (0.5 mL) at 0°C was added activated acid stock solution (see above) (3 mL, 0.08M in DCM, 0.24 mmol, 2.00 eq) and DMAP (3.1 mg, 25.0 μmol, 0.20 eq). The reaction was stirred for 30 minutes at room temperature. The reaction was quenched with half saturated $NH_4Cl$ solution (5 mL). After separation of the organic phase, the aqueous phase was extracted with DCM (2×5 mL). The combined organic layers were washed with brine (1×10 mL) and dried over $MgSO_4$ and concentrated *in vacuo*. Purification by column chromatography ($SiO_2$, CyHex/EtAc 10:1) gave ester **20** as a colourless oil (81.6 mg, 0.11 mmol, 88%).

$R_f$ = 0.64 (CyHex/EtAc 5:1); $[\alpha]_D^{20}$ = +23.8 (c=0.29, DCM); $^1$H-NMR (500 MHz, $CD_2Cl_2$): δ [ppm] = 6.42 (d, *J* = 15.1 Hz, 1H), 6.38 (ddt, *J* = 1.4, 10.8, 15.2 Hz, 1H), 6.36 (ddd, *J* = 0.6, 10.7, 17.4 Hz, 1H), 5.92 (d, *J* = 10.8 Hz, 1H), 5.92 (ddt, *J* = 6.9, 10.0, 17.2 Hz, 1H), 5.84 (s, 1H), 5.72 (dd, *J* = 6.7, 15.9 Hz, 1H), 5.64 (dt, *J* = 7.0, 14.6 Hz, 1H), 5.40 (d, *J* = 8.8 Hz, 1H), 5.14 (d, *J* = 17.5 Hz, 1H), 5.17-5.13 (m, 2H), 5.07 (dt, *J* = 1.4, 9.7 Hz, 1H), 4.99 (d, *J* = 10.8 Hz, 1H), 4.69 (d, *J* = 6.9 Hz, 1H), 4.25 (dd, *J* = 5.6, 9.0 Hz, 1H), 4.12 (t, *J* = 6.7 Hz, 2H), 3.35 (d, *J* = 9.9 Hz, 1H), 3.10 (s, 3H), 3.08 (dt, *J* = 1.4, 6.9 Hz, 2H), 2.44 (dt, *J* = 6.7, 6.7 Hz, 2H), 2.42 (m, 1H), 1.84 (d, *J* = 1.3 Hz, 3H), 1.79 (s, 3H), 1.71 (d, *J* = 1.2 Hz, 3H), 1.59 (m, 1H), 1.58 (s, 3H), 0.92 (s, 9H), 0.88 (d, *J* = 6.9 Hz, 3H), 0.85 (s, 9H), 0.63 (d, *J* = 7.0 Hz, 3H), 0.05 (s, 3H), 0.00 (s, 6H), −0.04 (s, 3H); $^{13}$C{$^1$H}-NMR (126 MHz, $CD_2Cl_2$): δ [ppm] = 171.8, 142.1, 135.8, 135.2, 134.6, 133.9, 133.33, 133.30, 132.4, 131.2, 129.8, 129.6, 129.5, 129.0, 128.3, 118.5, 112.1, 88.7, 73.2, 72.3, 64.4, 56.0, 43.3, 41.0, 39.6, 32.8, 26.3 (3×), 26.1 (3×), 25.1, 20.7, 18.7, 18.6, 15.6, 12.8,

10.9, 9.3, −3.5, −4.2, −4.7, −4.8; HRMS (ESI-TOF) m/z: $[M+Na]^+$ Calcd for $C_{44}H_{76}O_5Si_2Na^+$ 763.5123, found 763.5126.

**Archazolog 7**

A solution of ester **20** (15.0 mg, 20.2 µmol, 1.00 eq) in toluene (27.0 mL resulting in a 0.75 mM solution) was refluxed for 30 minutes. Then metathese catalyst **14** (1.6 mg, 2.02 µmol, 10 mol%) was added in toluene (0.5 mL). The solution was refluxed for 2 h and afterwards another portion of metatheses catalyst **14** (1.6 mg, 2.02 µmol, 10 mol%) was added in toluene (0.5 mL). The solution was refluxed for additional 2 h. Then the reaction was concentrated in vacuo. Purification by column chromatography ($SiO_2$, CyHex/EtAc 10:1) gave an undefined mixture of starting material, TBS-protected archazolog F (major) and minor stereoisomers. The ring closing was controlled by COSY NMR. For deprotection, the mixture was solved in THF (0.3 mL) and at 0°C pyridine (0.3 mL) and HF×pyridine (70%, 0.2 mL) was added subsequently. The reaction was stirred for 20 h at room temperature. Then the reaction was quenched at 0°C with pH 7 buffer solution (5 mL) and diluted with EtAc (5 mL). After separation of the organic phase, the aqueous phase was extracted with EtAc (3×2 mL). The combined organic layers were washed with a saturated $NaHCO_3$ solution (3 mL) and brine (3 mL). The organic layer was dried over MgSO 4 and concentrated in vacuo. Purification by column chromatography ($SiO_2$, CyHex/EtAc 3:1) gave a mixture of products which were further purified by HPLC (see SI section). Archazolog F (**7**) was obtained as a white solid (3.1 mg, 6.40 µmol, 32% over 2 steps).

$R_f$ = 0.33 (CyHex/EtAc 3:1); $[\alpha]_D^{20}$D = −51.5 (c=0.29, DCM); $^1$H-NMR (700 MHz, $CD_2Cl_2$): δ [ppm] = 6.56 (d, *J* = 16.1 Hz, 1H), 6.33 (ddt, *J* = 1.4, 10.8, 15.1 Hz, 1H), 6.01 (d, *J* = 15.5 Hz, 1H), 5.88 (d, *J* = 11.4 Hz, 1H), 5.73 (ddd, *J* = 6.1, 8.7, 15.3 Hz, 1H), 5.70 (dd, *J* = 4.6, 16.1, 1H), 5.63 (s, 1H), 5.55 (dt, *J* = 7.2, 15.1 Hz, 1H) 5.27 (d, *J* = 8.5 Hz, 1H), 5.21 (dt, *J* = 1.1, 9.9 Hz,

1H), 4.44 (brs, 1H), 4.37 (ddd, *J* = 5.4, 8.1, 10.9 Hz, 1H), 4.07 (ddd, *J* = 2.8, 9.2, 9.5 Hz, 1H), 3.99 (ddd, *J* = 4.4, 4.4, 10.9 Hz, 1H), 3.44 (d, *J* = 9.6 Hz, 1H), 3.17 (s, 3H), 3.08 (dd, *J* = 6.5, 15.3 Hz, 1H), 3.05 (d, *J* = 9.9, 1H), 2.98 (dd, *J* = 8.7, 15.3 Hz, 1H), 2.45 (m, 2H), 2.33 (ddq, *J* = 6.7, 9.8, 9.8, 1H), 2.11 (brs, 1H), 1.90 (d, *J* = 1.3 Hz, 3H), 1.82 (m, 1H), 1.80 (d, *J* = 1.3 Hz, 3H), 1.78 (s, 3H), 1.62 (d, *J* = 1.1 Hz, 3H), 0.71 (d, *J* = 6.8 Hz, 3H), 0.54 (d, *J* = 7.2 Hz, 3H); $^{13}C\{^{1}H\}$-NMR (176 MHz, $CD_2Cl_2$): δ [ppm] = 172.0, 138.2, 137.1, 135.3, 134.6, 133.8, 133.8, 132.5, 131.3, 131.2, 129.9, 129.0, 128.5, 128.0, 121.9, 89.5, 73.5, 73.2, 63.9, 56.3, 41.9, 41.0, 39.0, 33.2, 25.1, 20.4, 17.9, 13.4, 12.4, 10.9; HRMS (ESI-TOF) m/z: $[M+Na]^+$ Calcd for $C_{30}H_{44}O_5Na^+$ 507.3081, found 507.3085.

**V-ATPase Assays**

We evaluated the compounds for inhibition of purified V-ATPase holoenzyme from the midgut of the tobacco hornworm *Manduca sexta*. V-ATPase was purified according to published procedures.[26] Activity assays with *M. sexta* V-ATPase were carried out using 3 μg of protein in a final volume of 160 μl containing 50 mM Tris-MOPS (pH 8.1), 1 mM $MgCl_2$, 20 mM KCl, 5 mM Tris-HCl, 3 mM *β*-mercaptoethanol, 1 mM ATP and 6.25% dimethyl sulfoxide for archazolide samples or 1% ethanol for DCC samples, respectively. The inhibitors were diluted from 10 mM or 100 mM stocks in pure solvent, respectively and mixed with the sample. After 5 min of pre-incubation at 30 °C with or without inhibitors, 1 mM Tris-ATP was added and after incubation for 2 min the reaction was stopped by placing the tube in liquid nitrogen.To test the yeast V-ATPase activity, 3 μg of vacuolar protein were used in a final volume of 160 μl containing 50 mM Tris-MES pH 6.9, 3.75 mM $MgCl_2$, 0.1 mM sodium orthovanadate, 20 mM KCl, 0.5 mM sodium azide, 5 mM Tris-HCl, 2 mM ATP and 6.25% dimethyl sulfoxide for archazolide samples or 1% ethanol for DCC samples, respectively. In general, the samples were treated as described above, but incubation in the presence of ATP was carried out for 20 min. Inorganic phosphate produced in the

assays of V-ATPase, was measured according to the protocol of Wieczorek *et al*.[26,31] V-ATPase holoenzyme from *Manduca sexta* and from yeast vacuoles was obtained as previously described.[10]

**MTT assay**

The test compounds were investigated at human 1321N1 astrocytoma cells using the MTT (3-(4,5-dimethylthiazol-2-yl)-2,5-diphenyltetrazolium bromide) assay in order to assess their cytotoxic effects. ~~Cells were routinely checked for mycoplasma.~~ Assays were performed as previously described by Baqi *et al.*[25] In brief, cells were detached from the 175 $cm^2$ culture flasks in which they were grown, and subsequently counted using a Neubauer haemocytometer. Then they were resuspended in the growth medium. An aliquot of the cell suspension (180 µL) was added into each well of a 96-well plate to obtain 1000 cells per well, and incubated for 24 h at 37°C, 5% $CO_2$ and 95% humidity. The outer wells of the 96-well plate were filled with 200 µL PBS (phosphate-buffered saline) to prevent evaporation of the fluid. After 24 h stock solutions (10 mM) of the test compounds (archazolids and bafilomycin) were prepared in DMSO and diluted with cell culture medium to give 10-fold of the final concentrations. Then test compound solution (20 µL) was added to each well. The final DMSO concentration was 1%. For the standard compound 5-fluorouracil used as a control full concentration-inhibition curves were determined. The cells were incubated in the presence of the appropriate drug for 71 h. Then 40 µL from a freshly made stock solution of MTT (3-(4,5-dimethylthiazol-2-yl)-2,5-diphenyltetrazolium bromide)) in water (5 mg/mL) was added to each well and the cells were incubated for 1 h at 37°C, 5% $CO_2$. After the incubation time the medium containing MTT was removed and 100 µL of DMSO was added to each well in order to dissolve the crystals that were formed. The spectrophotometric absorbance was subsequently measured at 570 nm using a

FlexStation® (3 multimode plate reader, molecular devices) with a reference filter of 690 nm. The data were analyzed using Microsoft Excel and Graphpad Prism 5. Results were evaluated by comparing the absorbance of the wells containing compound-treated cells with the absorbance of wells containing 1% DMSO without any drug (= 100% viability). All experiments were performed in duplicates in at least 3 separate experiments.

**Calcium assays**

Measurement of intracellular $Ca^{2+}$ concentrations was performed in transfected 1321N1 astrocytoma cells as previously described.[32,33] The human (h) P2 nucleotide receptor subtypes hP2X2, hP2X4, hP2X7, $hP2Y_1$, $hP2Y_2$, $hP2Y_4$, $hP2Y_6$ and $hP2Y_{11}$ were activated with the appropriate agonist, and agonist-induced increases in intracellular $Ca^{2+}$ concentration and their inhibition by test compounds were measured. The fluorescent $Ca^{2+}$-chelating dye FLUO-4 was used as an indicator of the intracellular $Ca^{2+}$ levels except for P2X1 and P2X3 receptor assays (see below). The experiments were performed in 96-well plates using a fluorescence imaging plate reader (Novostar, BMG, Germany). Cells were grown to confluence in 96-well black-walled tissue culture plates and loaded with FLUO-4 AM (2.4 μM) in Hank's balanced salt solution (HBSS, containing 10 mM HEPES, pH 7.3, and 1% Pluronic® F127) for 1 h at 23°C. After incubation the loaded cells were washed with the same buffer to remove extracellular FLUO-4 AM. Test compound solutions were prepared in DMSO and added 30 min before the addition of the agonist. The final DMSO concentration in the assays did not exceed 1%. Fluorescence intensity was measured at 520 nm for 30 s at 0.4 s intervals. Buffer, or agonist solution at a concentration equal to its $EC_{80}$ value, were injected sequentially into separate wells using the automatic pipetting device of the instrument. The assays were performed in a final volume of 200 μl.

For hP2X1 and hP2X3 receptors the assays were performed in the same way with the exception that calcium 5 was used as a dye. The loaded cells were incubated for 1 h at 37 °C, and after incubation, the dye was removed and buffer with or without test compound was added to the cells without previous washing.

Calcium mobilization assays at the human GPR17 were performed according to published procedures.[34] Cells expressing the hGPR17 were harvested with 0.05 % trypsin / 0.02 % EDTA and rinsed with culture medium. The cells were kept under 5 % $CO_2$ at 37°C for 45 min and then centrifuged at 200 x g and 4°C for 5 min. After that the cells were incubated for 1 h at 25°C in Krebs-Ringer-HEPES buffer, pH 7.4 containing 3 µM Oregon Green BAPTA-1/AM and 1 % Pluronic®F127. The cells were rinsed three times with KRH buffer, diluted and plated into 96-well plates with clear bottoms at a density of approximately 16,000 cells/well and left for 30 min. Then the assay was performed as described above for the other receptors.

**$A_3$ adenosine receptor radioligand binding assay**

Membrane preparations of Chinese hamster ovary (CHO) cells expressing human $A_3$ARs were obtained as described before.[34] [$^3$H]Phenyl-8-ethyl-4-methyl-(8*R*)-4,5,7,8-tetrahydro-1*H*-imidazo[2,1-*i*]purine-5-one ([$^3$H]PSB-11, 53 Ci/mmol) was used as a radioligand (0.5 nM).[35] Nonspecific binding was determined in the presence of 100 µM (*R*)-N$^6$-phenylisopropyladenosine (*R*-PIA). The competition assays were performed in a total volume of 400 µl in assay buffer (50 mM TRIS-HCl, pH 7.4). Stock solutions of the test compounds were prepared in DMSO; the final DMSO concentration was 1%. The membrane preparations were preincubated for 20 min with adenosine deaminase (ADA) 2 U/mL per mg of protein. Incubation was carried out for 60 min at 23°C. The incubation was terminated by filtration through GF/B glass fiber filters using a 48-channel cell harvester, and filters were washed three times with ice-

cold TRIS-HCl buffer (50 mM, pH 7.4).The filters were transferred into scintillation vials and incubated for 6 h with 2.5 mL of scintillation cocktail (Beckman Coulter). Radioactivity was counted in a liquid scintillation counter. At least three separate experiments were performed. Data were analyzed using Graph Pad Prism version 5 (San Diego, CA, USA). For the calculation of $K_i$ values by nonlinear regression analysis, the Cheng-Prusoff equation and a $K_D$ value of 4.9 nM for [$^3$H]PSB-11 was used.

**Radioligand binding studies at human P2X3 receptors**

Assays were performed as described previously.[36] Membrane preparations of astrocytoma cells expressing the hP2X3 receptor were obtained and used for competition binding studies. Compound dilutions were prepared in DMSO; the final DMSO concentration was 1%. Assays were performed in assay buffer (50 mM Tris-HCl, pH 7.4) containing 1 mM EDTA and 0.2 nM [$^{35}$S]ATPγS. The incubations were started by the addition of membranes (50 μg) and were performed in an assay volume of 500 μL. The reactions were terminated by vacuum filtration over GF/B glass-fiber filters using a Brandel 48-well harvester and the samples were further treated as described above for $A_3$ adenosine receptor binding assays.

**Blood-brain barrier permeation**

Permeation experiments were carried out in a 96-well Multiscreen Immobilon® (donor plate), inserted in a 96-well tray as acceptor plate. The hydrophobic filter material of the Immobilon® plate was pre-wetted with 70% aq. EtOH and treated with a solution of lipids (brain polar lipid extract dissolved in 1.9-decadiene). The acceptor plate was filled with Tris buffer and both plates were inserted into each other and placed onto an orbital shaker for 40 min at 100 rpm. The transport study was started by applying the test compounds at a concentration of 10 μM, and solutions of reference compounds, to the donor plate. After 16.0 ± 0.5 h of diffusion at rt, the

contents of the acceptor and donor plate and the starting solutions were collected and quantified by LC/MS.

**Caco2 transport screening**

For transport studies Caco-2 cells were differentiated for 21 days in Transwell® plates. Bidirectional permeation experiments were performed. Compounds were tested at a concentration of 10 μM.

**Plasma protein binding**

Plasma-protein binding was measured using Li-heparin plasma obtained from mice (CD-1, male, pooled), rat (SD, male, pooled) and humans (mixed gender, pooled). Compounds were tested at a concentration of 1 μM using ultrafiltration.

**Microsomal stability**

Pooled liver microsomes (0.5 mg/ml) from mouse (CD-1, male, pooled), rat (SD, male, pooled) or human (mixed gender, pooled) were employed. Compounds were tested at a concentration of 1 μM.

**CYP inhibition**

Effects of test compounds on single recombinant CYP enzymes relevant for drug metabolism (CYP1A2, CYP2B6, CYP2C9, CYP2C19, CYP2D6 and CYP3A4) were investigated. Compounds were tested at a concentration of 1 μM.

**Protease assays**

The spectrophotometric inhibition assays for five proteases were performed with chromogenic peptide substrates, which, upon cleavage, release *para*-nitroaniline (pNA). Progress curves were followed over 10 min (HLE, trypsin), 1 h (cathepsins B and L) or 12.5 min (chymotrypsin), monitored at 405 nm and analyzed by linear regression. No inhibition related to more than 95%

activity in duplicate measurements at a single inhibitor concentration ≥ 1 μM. $IC_{50}$ values were determined from duplicate measurements by nonlinear regression using equation $v_s = v_0/(1 + [I]/IC_{50})$, where $v_s$ is the steady-state rate, $v_0$ is the rate in the absence of the inhibitor, and [I] is the inhibitor concentration. Standard errors of the mean refer to the non-linear regression analysis. HLE was assayed at 25°C with MeO-Suc-Ala-Ala-Pro-Val-pNA at a substrate concentration of 100 μM (1.85 × $K_m$).[37] A modified assay was applied.38 Cathepsins B and L were assayed at 37 °C with 500 μM (0.45 × $K_m$) Z-Arg-Arg-pNA and 100 μM Z-Phe-Arg-pNA (5.88 × $K_m$) respectively.[39] Chymotrypsin was assayed at 25°C with 200 μM (2.68 × $K_m$) Suc-Ala-Ala-Pro-Phe-pNA.[37] Trypsin was assayed at 25°C with 200 μM (2.70 × $K_m$) Suc-Ala-Ala-Pro-Arg-pNA.[40]

**Kinase assays**

These studies were performed by DiscoverX Corporation (42501 Albrae Street, Fremont, CA 94538-3142, www.discoverx.com). For most assays, kinase-tagged T7 phage strains were grown in parallel in 24-well blocks in an *E. coli* host derived from the BL21 strain. *E. coli* were grown to log-phase and infected with T7 phage from a frozen stock (multiplicity of infection = 0.4) and incubated with shaking at 32°C until lysis (90-150 minutes). The lysates were centrifuged (6,000×g) and filtered (0.2 μm) to remove cell debris. The remaining kinases were produced in HEK-293 cells and subsequently tagged with DNA for qPCR detection. Streptavidin-coated magnetic beads were treated with biotinylated small molecule ligands for 30 minutes at room temperature to generate affinity resins for kinase assays. The liganded beads were blocked with excess biotin and washed with blocking buffer (SeaBlock (Pierce), 1% BSA, 0.05 % Tween 20, 1 mM DTT) to remove unbound ligand and to reduce non-specific phage binding. Binding reactions were assembled by combining kinases, liganded affinity beads, and test compounds in

1x binding buffer (20% SeaBlock, 0.17x PBS, 0.05% Tween 20, 6 mM DTT). Test compounds were prepared as 40x stocks in 100% DMSO and directly diluted into the assay. All reactions were performed in polypropylene 384-well plates in a final volume of 0.02 ml. The assay plates were incubated at room temperature with shaking for 1 hour and the affinity beads were washed with wash buffer (1x PBS, 0.05 % Tween 20). The beads were then re-suspended in elution buffer (1x PBS, 0.05 % Tween 20, 0.5 μM non-biotinylated affinity ligand) and incubated at room temperature with shaking or 30 minutes. The kinase concentration in the eluates was measured by qPCR.

## ASSOCIATED CONTENT

**Supporting Information**.

The Supporting Information is available free of charge on theACS Publications website at DOI:…

Synthetic scheme and experimental procedure for all compounds, additional structure activity data, bio-chemical and cellular assay conditions, full NMR assignment for all compounds, HPLC chromatograms, and copies of NMR data (PDF). Molecular formula strings (CSV)

## AUTHOR INFORMATION

**Corresponding Author**

* E-mail: dirk.menche@uni-bonn.de. Phone (+49)228-732653. Fax: (+49)228-735813.

E-mail: christa.mueller@uni-bonn.de. Phone (+49)228-73-2301. Fax: (+49) 228-732567.

Christa E. Müller: orcid.org/0000-0002-0013-6624

**Author Contributions**

The manuscript was written through contributions of all authors. All authors have given approval to the final version of the manuscript.

ACKNOWLEDGMENTS

Generous financial support by the Deutsche Forschungsgemeinschaft (DFG, German Research Foundation) – Project-IDs: Forschergruppe 1406, SFB 431 and TRR 261 (B07) and the BMBF (Neuroallianz project T7B) is most gratefully acknowledged. We thank Andreas J. Schneider (University of Bonn) for excellent HPLC-support, Martin Dransmann and Katharina Sylvester for excellent technical assistance and Dr. Sebastian Essig and Simon Dedenbach for early synthetic studies.

ABBREVIATIONS USED

BuLi, n-butyllithium; EtOAc, ethyl acetate; FXR, farnesoid X receptor; HLE, human leukocyte elastase; KHMDS, potassium bis(trimethylsilyl)amide; MDM2, mouse double minute 2 homolog; mPGES-1, microsomal prostaglandin E synthase; P2X, P2X purinoceptor; P2Y, P2Y purinoceptor; PAMPA, parallel artificial permeation assay; rt, room temperature; V-ATPase, vacuolar type ATPase;

REFERENCES

[1] a) Beyenbach, K. W.; Wieczorek, H. The V-type $H^+$ ATPase: molecular structure and function, physiological roles and regulation. *J. Exp. Biol.* **2006**, *209*, 577-589; b) Jefferies, K. C.; Cipriano, D. J.; Forgac, M. Function, structure and regulation of the vacuolar ($H^+$)-ATPases.

*Arch. Biochem. Biophys.* **2008**, *476*, 33-42; c) Cotter, K.; Stransky, L.; McGuire, C.; Forgac, M. Recent insights into the structure, regulation, and function of the V-ATPases. *Trends Biochem. Sci.* **2015**, *40*, 611-622.

[2] a) Maxfield, F. R.; McGraw, T. E. Endocytic recycling. *Nat. Rev. Mol. Cell Biol.* **2004**, *5*, 121-132; b) Hiesinger, P. R.; Fayyazuddin, A.; Mehta, S. Q.; Rosenmund, T.; Schulze, T. L.; Zhai, R. G.; Verstreken, P.; Cao, Y.; Zhou, Y.; Kunz, J.; Bellen, H. J. The V-ATPase $V_0$ subunit a1 is required for a late step in synaptic vesicle exocytosis in Drosophila. *Cell* **2005**, *121*, 607-620.

[3] Brown, D; Paunescu, T.G.; Breton, S.; Marshansky, V. Regulation of the V-ATPase in kidney epithelial cells: dual role in acid-base homeostasis and vesicle trafficking. *J. Exp. Biol.* **2009**, *212*, 1762-1772.

[4] Toyomura, T.; Murata, Y.; Yamamoto, A.; Oka, T.; Sun-Wada, G. H.; Wada, Y.; Futai, M. From lysosomes to the plasma membrane - Localization of vacuolar type $H^+$-ATPase with the a3 isoform during osteoclast differentiation. *J. Biol. Chem.* **2003**, *278*, 22023-22030.

[5] Pietrement, C.; Sun-Wada, G. H.; Silva, N. D.; McKee, M.; Marshansky, V.; Brown, D.; Futai, M.; Breton, S. Distinct expression patterns of different subunit Isoforms of the V-ATPase in the rat epididymis. *Biol. Reprod.* **2006**, *74*, 185-194.

[6] Hamm, R.; Chen, Y. R.; Seo, E. J.; Zeino, M.; Wu, C. F.; Müller, R.; Yang, N. S.; Efferth, T. Induction of cholesterol biosynthesis by archazolid B in T24 bladder cancer cells. *Biochem. Pharmacol.* **2014**, *91*, 18-30.

[7] Scherer, O.; Steinmetz, H.; Kaether, C.; Weinigel, C.; Barz, D.; Kleinert, H.; Menche, D.; Müller, R.; Pergola, C.; Werz, O. Targeting V-ATPase in primary human monocytes by archazolid potently represses the classical secretion of cytokines due to accumulation at the endoplasmic reticulum. *Biochem. Pharmacol.* **2014**, *91*, 490-500.

[8] For reviews, see: a) Forgac, M. Vacuolar ATPases: rotary proton pumps in physiology and pathophysiology. *Nat. Rev. Mol. Cell Biol.* **2007**, *8*, 917-929; b) Huss, M.; Wieczorek, H. Inhibitors of V-ATPases: old and new players. *J. Exp. Biol.* **2009**, *212*, 341-346.

[9] a) Sasse, F.; Steinmetz, H.; Höfle, G.; Reichenbach, H. Archazolids, new cytotoxic macrolactones from *Archangium gephyra* (myxobacteria) - Production, isolation, physico-chemical and biological properties. *J. Antibiot.* **2003**, *56*, 520-525; b) Huss, M.; Sasse, F.; Kunze, B.; Jansen, R.; Steinmetz, H.; Ingenhorst, G.; Zeeck, A.; Wieczorek, H. Archazolid and apicularen: Novel specific V-ATPase inhibitors. *BMC Biochem.* **2005**, *6*, 13.

[10] Bockelmann, S.; Menche, D.; Rudolph, S.; Bender, T.; Grond, S.; von Zezschwitz, P.; Muench, S. P.; Wieczorek, H.; Huss, M. Archazolid A binds to the equatorial region of the c-ring of the vacuolar $H^+$-ATPase *J. Biol. Chem.* **2010**, *285*, 38304-38314.

[11] Gölz, J. P.; Bockelmann, S.; Mayer, K.; Steinhoff, H.-J. Wieczorek, H.; Huss, M.; Klare, J. P.; Menche, D. EPR studies of V-ATPase with spin-labeled inhibitors DCC and archazolid: interaction dynamics with proton translocating subunit c *ChemMedChem* **2016**, *11*, 420-428.

[12] a) Wiedmann, R. M.; von Schwarzenberg, K.; Palamidessi, A.; Schreiner, L.; Kubisch, R.; Liebl, J.; Schempp, C.; Trauner, D.; Vereb, G.; Zahler, S.; Wagner, E.; Müller, R.; Scita, G.; Vollmar, A. M. The V-ATPase-inhibitor archazolid abrogates tumor metastasis via inhibition of endocytic activation of the Rho-GTPase Rac1. *Cancer Res.* **2012**, *72*, 5976-5987; b) Von

Schwarzenberg, K.; Wiedmann, R. M.; Oak, P.; Schulz, S.; Zischka, H.; Wanner, G.; Efferth, T.; Trauner, D.; Vollmar, A. M. Mode of cell death induction by pharmacological vacuolar $H^+$-ATPase (V-ATPase) inhibition. *J. Biol. Chem.* **2013**, *288*, 1385-1396; c) Kubisch, R.; Fröhlich, T.; Arnold, G. J.; Schreiner, L; von Schwarzenberg, K.; Roidl, A.; Vollmar, A. M.; Wagner, E. V-ATPase inhibition by archazolid leads to lysosomal dysfunction resulting in impaired cathepsin B activation in vivo. *Int. J. Cancer* **2014**, *134*, 2478–2488; d) Schempp, C. M.; von Schwarzenberg, K.; Schreiner, L.; Kubisch, R.; Müller, R.; Wagner, E.; Vollmar, A. M. V-ATPase inhibition regulates anoikis resistance and metastasis of cancer cells. *Mol. Cancer Ther.* **2014**, *13*, 926-937; e) Von Schwarzenberg, K.; Lajtos, T.; Simon, L.; Müller, R.; Vereb, G.; Vollmar, A. M. V-ATPase inhibition overcomes trastuzumab resistance in breast cancer. *Mol. Oncol.* **2014**, *8*, 9-19; f) Schneider, L. S.; von Schwarzenberg, K.; Lehr, T.; Ulrich, M.; Kubisch-Dohmen, R.; Liebl, J.; Trauner, D.; Menche, D.; Vollmar, A. M. Vacuolar-ATPase inhibition blocks iron metabolism to mediate therapeutic effects in breast cancer. *Cancer Res.* **2015**, *75*, 2863-2874; g) Schneider, L. S.; Ulrich, M.; Lehr, T.; Menche, D.; Müller, R.; von Schwarzenberg, K. MDM2 antagonist nutlin-3a sensitizes tumors to V-ATPase inhibition. *Mol. Oncol.* **2016**, *10*, 1054-1062; h) Thomas, L.; Rao, Z.G.; Gerstmeier, J.; Raasch, M.; Weinigel, C.; Rummler, S.; Menche, D.; Müller, R.; Pergola, C.; Mosig, A.; Werz, O. Selective upregulation of TNFα, expression in classically-activated human monocyte-derived macrophages (M1) through pharmacological interference with V-ATPase. *Biochem. Pharmacol.* **2017**, *130*, 71-82; i) Bartel, K.; Winzi, M.; Ulrich, M.; Koeberle, A.; Menche, D.; Werz, O.; Müller, R.; Guck, J.; Vollmar, A. M.; von Schwarzenberg, K. V-ATPase inhibition increases cancer cell stiffness and blocks membrane related Ras signaling - a new option for HCC therapy. *Oncotarget* **2017**, *8*, 9476-9487; j) Luong, B.; Schwenk, R.; Bräutigam, J.; Müller, R.; Menche, D.; Bischoff, I.; Fürst, R.

The vacuolar-type ATPase inhibitor archazolid increases tumor cell adhesion to endothelial cells by accumulating extracellular collagen. *PLOS ONE* **2018**, *13*, e0203053.

[13] a) Pérez-Sayáns, M.; Somoza-Martín, J. M.; Barros-Angueira, F.; Gándara Rey, J. M.; García-García, A. V-ATPase inhibitors and implication in cancer treatment. *Cancer Treat. Rev.* **2009**, *35*, 707-713; b) Hernandez, A.; Serrano-Bueno, G.; Perez-Castineira, J. R.; Serrano, A. Intracellular proton pumps as targets in chemotherapy: V-ATPases and cancer. *Curr. Pharm. Des.* **2012**, *18*, 1383-1394; c) Cotter, K.; Capecci, J.; Sennoune, S.; Huss, M.; Maier, M.; Martinez-Zaguilan, R.; Forgac, M. Activity of plasma membrane V-ATPases is critical for the invasion of MDA-MB231 breast cancer cells. *J. Biol. Chem.* **2015**, *290*, 3680-3692.

[14] a) Menche, D.; Hassfeld, J.; Sasse, F.; Huss, M.; Wieczorek, H. Design, synthesis, and biological evaluation of novel analogues of archazolid: A highly potent simplified V-ATPase inhibitor. *Bioorg. Med. Chem. Lett.* **2007**, *17*, 1732-1735; b) Menche, D.; Hassfeld, J.; Steinmetz, H.; Huss, M.; Wieczorek, H.; Sasse, F. The first hydroxylated archazolid from the myxobacterium *Cystobacter violaceus*: Isolation, structural elucidation and V-ATPase inhibition. *J. Antibiot.* **2007**, *60*, 328-331; c) Menche, D.; Hassfeld, J.; Steinmetz, H.; Huss, M.; Wieczorek, H.; Sasse, F. Archazolid-7-O-beta-D-glucopyranoside - Isolation, structural elucidation and solution conformation of a novel V-ATPase inhibitor from the myxobacterium *Cystobacter violaceus*. *Eur. J. Org. Chem.* **2007**, *2007*, 1196–1202; d) Moulin, E.; Nevado, C.; Gagnepain, J.; Kelter, G.; Fiebig, H.-H.; Fürstner, A. Synthesis and evaluation of an Iejimalide-archazolid chimera. *Tetrahedron* **2010**, *66*, 6421-6428; e) Tran, A. B.; Melly, G. C.; Doucette, R.; Ashcraft, B.; Sebren, L. J.; Havko, N.; Young, J. C.; O'Neil, G. W. Synthesis and activity of the archazolid western hemisphere. *Org. Biom. Chem.* **2011**, *9*, 7671-7674; f) Persch, E.; Basile, T.; Bockelmann, S.; Huss, M.; Wieczorek, H.; Carlomagno, T.; Menche, D. Synthesis and biological

evaluation of a water-soluble derivative of the potent V-ATPase inhibitor archazolid. *Bioorg. Med. Chem. Lett.* **2012**, *22*, 7735-7738; g) Dreisigacker, S.; Latek, D.; Bockelmann, S.; Huss, M.; Wieczorek, H.; Filipek, S.; Gohlke, H.; Menche, D.; Carlomagno, T. Understanding the inhibitory effect of highly potent and selective archazolides binding to the vacuolar ATPase. *J. Chem. Inf. Model.* **2012**, *52*, 2265-2272.

[15] Reker, D.; Perna, A. M.; Rodrigues, T.; Schneider, P.; Reutlinger, M.; Mönch, B.; Koeberle, A.; Lamers, C.; Gabler, M.; Steinmetz, H.; Müller, R.; Schubert-Zsilavecz, M.; Werz, O.; Schneider, G. Revealing the macromolecular targets of complex natural products. *Nat. Chem.* **2014**, *6*, 1072-1078.

[16] Horstmann, H.; Essig, S.; Bockelmann, S.; Wieczorek, H.; Huss, M.; Sasse, F.; Menche, D. Archazolid A-15-O-beta-D-glucopyranosilde and iso-archazolid B: Potent V-ATPase inhibitory polyketides from the myxobacteria *Cystobacter violaceus* and *Archangium gephyra. J. Nat. Prod.* **2011**, *74*, 1100-105.

[17] For total syntheses of archazolids, see: a) Menche, D.; Hassfeld, J.; Li, J.; Rudolph, S. Total synthesis of archazolid A. *J. Am. Chem. Soc.* **2007**, *129*, 6100-6101; b) Roethle, P. A.; Chen, I. T.; Trauner, D. Total synthesis of (-)-archazolid B. *J. Am. Chem. Soc.* **2007**, *129*, 8960-8961; c) Menche, D.; Hassfeld, J.; Li, J.; Mayer, K.; Rudolph, S. Modular total synthesis of archazolid A and B. *J. Org. Chem.* **2009**, *74*, 7220-7229; d) Scheeff, S.; Menche, D. Total synthesis of archazolid F. *Org. Lett.* **2019**, *21*, 271-274; e) for a review see: Scheeff, S.; Menche, D. Total syntheses of the archazolids: an emerging class of novel anticancer drugs. *Beilstein J. Org. Chem.* **2017**, *13*, 1085-1098.

[18] O'Neil, G.; Craig, A.; Williams, J.; Young, J.; Spiegel, P. Synthesis of the C-1-C-23 fragment of the archazolids and evidence for V-ATPase but not COX inhibitory activity. *Synlett* **2017**, *28*, 1101-1105.

[19] Hassfeld, J.; Farès, C.; Steinmetz, H.; Carlomagno, T.; Menche, D. Stereochemical determination of archazolid A and B, highly potent vacuolar-type ATPase inhibitors from the myxobacterium *Archangium gephyra*. *Org. Lett.* **2006**, *8*, 4751-4754.

[20] Kusebauch, B.; Busch, B.; Scherlach, K.; Roth, M.; Hertweck, C. Functionally distinct modules operate two consecutive α,β→β,γ double-bond shifts in the rhizoxin polyketide assembly line. *Angew. Chem. Int. Ed.* **2010**, *49*, 1460-1464.

[21] Stewart, I.C.; Ung, T.; Pletnev, A. A.; Berlin, J. M.; Grubbs, R. H.; Schrodi, Y. Highly efficient ruthenium catalysts for the formation of tetrasubstituted olefins via ring-closing metathesis. *Org. Lett.* **2007**, *9*, 1589-1592.

[22] Maier, M. E. Design and synthesis of analogues of natural products. *Org. Biomol. Chem.* **2015**, *13*, 5302–5343 [23] Borea, P. A.; Varani, K.; Vincenzi, F.; Baraldi, P. G.; Tabrizi, M. A.; Merighi, S.; Gessi, S. The A(3) adenosine receptor: History and perspectives. *Pharmacol. Rev.* **2015**, 67, 74-102.

[24] Maynard, J.P.; Lee, J. S.; Sohn, B. H.; Yu, X.; Lopez-Terrada, D.; Finegold, M. J.; Goss, J. A.; Thevananther S. P2X3 purinergic receptor overexpression is associated with poor recurrence-free survival in hepatocellular carcinoma patients. *Oncotarget* **2015**, *6*, 41162-41179.

[25] Baqi, Y.; Atzler, K.; Köse, M.; Glänzel, M.; Müller, C. E. High-Affinity, non-nucleotide-derived competitive antagonists of platelet P2Y(12) receptors. *J. Med. Chem.* **2009**, *25*, 3784–37893.

[26] Huss, M.; Ingenhorst, G.; König, S.; Gassel, M.; Dröse, S.; Zeeck, A.; Altendorf, K.; Wieczorek, H. Concanamycin a, the specific inhibitor of V-ATPases, binds to the V-o subunit c. *J. Biol. Chem.* **2002**, *277*, 40544-40548.

[27] Mansoor, S. E.; Lü, W.; Oosterheert, W.; Shekhar, M.; Tajkhorshid, E.; Gouaux, E. X-ray structures define human P2X3 receptor gating cycle and antagonist action *Nature* **2016,** *538*, 66–71.

[28] Müller, C. E. Medicinal chemistry of P2X receptors: allosteric modulators. *Curr. Med. Chem.* **2015**, *22*, 929-941.

[29] Fulmer, G. R.; Miller, A. J. M.; Sherden, N. H.; Gottlieb, H. E.; Nudelman, A.; Stoltz, B. M.; Bercaw, J. E.; Goldberg, K. I. NMR chemical shifts of trace impurities: common laboratory solvents, organics, and gases in deuterated solvents relevant to the organometallic chemist. *Organometallics* **2010**, *29*, 2176–2179.

[30] Zhang, W.; Bah, J.; Wohlfarth, A.; Franzen, J. A stereodivergent strategy for the preparation of corynantheine and ipecac alkaloids, their epimers, and analogues: efficient total synthesis of (-)-dihydrocorynantheol, (-)-corynantheol, (-)-protoemetinol, (-)-corynantheal, (-)-protoemetine, and related natural and nonnatural compounds. *Chem. Eur. J.* **2011**, *17*, 13814–13824.

[31] Wieczorek, H; Cioffi, M.; Klein, U.; Harvey, W. R.; Schweikl, H.; Wolfersberger, M. G. Isolation of goblet cell apical membrane from tobacco hornworm midgut and purification of its vacuolar-type ATPase.*Methods Enzymol.* **1990**, *192*, 608–616.

[32] Abdelrahman, A.; Namasivayama, V.; Hinz, S.; Schiedel, A. C.; Köse, M.; Burton, M.; El-Tayeb, A.; Gillard, M.; Bajorath, J.; de Ryck, M.; Müller, C. E. Characterization of P2X4 receptor agonists and antagonists by calcium influx and radioligand binding studies *Biochem. Pharmacol.* **2017**, *125*, 41-54.

[33] Rafehi, M.; Burbiel, J. C.; Attah, I. Y.; Abdelrahman, A.; Müller, C. E. Synthesis, characterization, and in vitro evaluation of the selective $P2Y_2$ receptor antagonist AR-C118925 *Purinergic Signalling* **2017**, *13*, 89-103.

[34] Hillmann, P.; Ko, G. Y.; Spinrath, A.; Raulf, A.; von Kügelgen, I.; Wolff, S. C.; Nicholas, R. A.; Kostenis, E.; Höltje, H. D.; Müller, C. E. Key determinants of nucleotide-activated g protein-coupled P2Y(2) receptor function revealed by chemical and pharmacological experiments, mutagenesis and homology modeling. *J. Med. Chem.* **2009**, *52*, 2762–2775.

[35] Müller, C. E.; Diekmann, M.; Thorand, M.; Ozola, V. [H-3]8-ethyl-4-methyl-2-phenyl-(8*R*)-4,5,7,8-tetrahydro-1H-imidazo[2,1-i]-purin-5-one ([H-3]PSB-11), a novel high-affinity antagonist radioligand for human A(3) adenosine receptors. *Bioorg. Med. Chem. Lett.* **2002**, *12*, 501–503.

[36] Hernandez-Olmos, V.; Abdelrahman, A.; El-Tayeb, A.; Freudendahl, D.; Weinhausen, S.; Müller, C. E. N-substituted phenoxazine and acridone derivatives: structure-activity relationships of potent P2X4 receptor antagonists. *J. Med. Chem.* **2012**, *55*, 9576–9588.

[37] Gütschow, M.; Pietsch, M.; Themann, A.; Fahrig, J.; Schulze, B. 2,4,5-triphenylisothiazol-3(2H)-one 1,1-dioxides as inhibitors of human leukocyte elastase. *J. Enz. Inhib. Med. Chem.* **2005**, *20*, 341–347.

[38] Steinebach, C.; Schulz-Fincke, A. C.; Schnakenburg, G.; Gütschow, M. In situ generation and trapping of thioimidates: an intermolecular tandem reaction to 4-acylimino-4H-3,1-benzothiazines. *RSC Adv.* **2016**, *6*, 15430–15440.

[39] Frizler, M.; Lohr, F.; Lülsdorff, M.; Gütschow, M. Facing the gem-dialkyl effect in enzyme inhibitor design: preparation of homocycloleucine-based azadipeptide nitriles. *Chem. Eur. J.* **2011**, *17*, 11419–11423.

[40] Sisay, M. T.; Steinmetzer, T.; Stirnberg, M.; Maurer, E.; Hammami, M.; Bajorath, J.; Gütschow, M. Identification of the first low-molecular-weight inhibitors of matriptase-2. *J. Med. Chem.* **2010**, *53*, 5523–5535.

## ToC Graphic

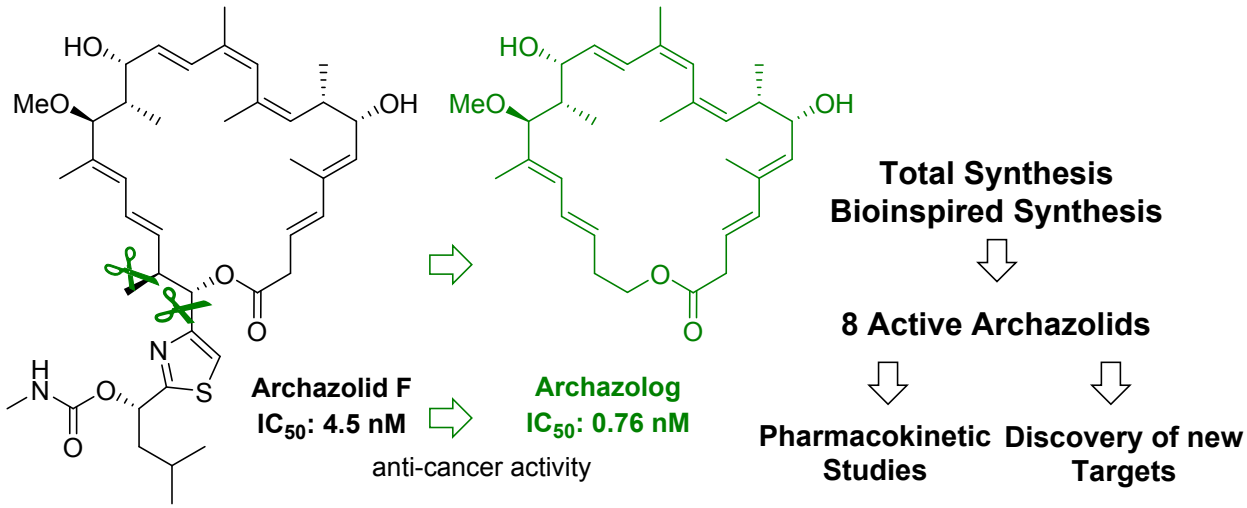
HO
MeO
OH
O
O
N
S
H
N
O
O
Archazolid F
IC50: 4.5 nM
anti-cancer activity
HO
MeO
OH
O
O
Archazolog
IC50: 0.76 nM
Total Synthesis
Bioinspired Synthesis
8 Active Archazolids
Pharmacokinetic Studies
Discovery of new Targets